AD_____

AWARD NUMBER: W81XWH-07-1-0153

TITLE: Examination of the Role of DNA Methylation Changes in Prostate Cancer using the Transgenic Adenocarcinoma of Mouse Prostate (TRAMP) Model

PRINCIPAL INVESTIGATOR: Shannon R. Morey Kinney, Ph.D.

CONTRACTING ORGANIZATION: Roswell Park Cancer Institute
Buffalo, NY 14263

REPORT DATE: March 2010

TYPE OF REPORT: Annual Summary

PREPARED FOR: U.S. Army Medical Research and Materiel Command
Fort Detrick, Maryland 21702-5012

REPORT DOCUMENTATION PAGE

Form Approved
OMB No. 0704-0188

1. REPORT DATE	2. REPORT TYPE	3. DATES COVERED
1 March 2010	Annual Summary	1 Mar 2007 – 28 Feb 2010

4. TITLE AND SUBTITLE

Examination of the Role of DNA Methylation Changes in Prostate Cancer using the Transgenic Adenocarcinoma of Mouse Prostate (TRAMP) Model

5a. CONTRACT NUMBER

5b. GRANT NUMBER
W81XWH-07-1-0153

5c. PROGRAM ELEMENT NUMBER

6. AUTHOR(S)

Shannon R. Morey Kinney, Ph.D.

E-Mail: kinney@neb.com

5d. PROJECT NUMBER

5e. TASK NUMBER

5f. WORK UNIT NUMBER

7. PERFORMING ORGANIZATION NAME(S) AND ADDRESS(ES)

Roswell Park Cancer Institute
Buffalo, NY 14263

8. PERFORMING ORGANIZATION REPORT NUMBER

9. SPONSORING / MONITORING AGENCY NAME(S) AND ADDRESS(ES)
U.S. Army Medical Research and Materiel Command
Fort Detrick, Maryland 21702-5012

10. SPONSOR/MONITOR'S ACRONYM(S)

11. SPONSOR/MONITOR'S REPORT NUMBER(S)

12. DISTRIBUTION / AVAILABILITY STATEMENT
Approved for Public Release; Distribution Unlimited

13. SUPPLEMENTARY NOTES

14. ABSTRACT
I have characterized the epigenetic changes that occur throughout tumor progression in the Transgenic Adenocarcinoma of Mouse Prostate (TRAMP) mouse model. In addition, I examined the role of Dnmt1 in normal prostate development and TRAMP tumorigenesis. TRAMP tumors display altered DNA methyltransferase (Dnmt) expression and DNA methylation patterns, such that global DNA hypomethylation occurs early, while locus specific DNA hypermethylation occurs late, during TRAMP tumor progression. We have identified a number of genes that are promoter hypermethylation events in TRAMP tumors. Interestingly, several loci display a unique phenomenon of gene body methylation correlating with increased expression. While Dnmt1 hypomorphic mouse prostates develop normally, decreased Dnmt1 expression in TRAMP mice (TRAMP Dnmt1 hypomorphic mice) leads to advanced tumor progression at early time points and repressed tumor development and metastases at a later time point. These results suggest that both global hypomethylation and locus specific hypermethylation are important events during TRAMP tumorigenesis and that Dnmt1 plays a dual role in TRAMP tumor progression with a suppressive function in early stage disease and oncogenic function at later stages.

15. SUBJECT TERMS
Prostate cancer, DNA methylation, Transgenic Adenocarcinoma of Mouse Prostate (TRAMP)

16. SECURITY CLASSIFICATION OF:			17. LIMITATION OF ABSTRACT	18. NUMBER OF PAGES	19a. NAME OF RESPONSIBLE PERSON
a. REPORT	b. ABSTRACT	c. THIS PAGE			19b. TELEPHONE NUMBER *(include area code)*
U	U	U	UU	37	USAMRMC

Table of Contents

Introduction:

DNA hypermethylation of tumor suppressor gene promoters, in conjunction with hypomethylation of repetitive elements and increased expression of DNA methyltransferases (DNMTs), occurs in human prostate cancer. An understanding of how DNA methylation becomes deregulated in prostate cancer and how to reverse or prevent this process is important for developing anticancer therapies. It has also been shown that pharmacological inhibition of DNMTs can have anticancer effects, supporting the concept that hypomethylation and thus re-expression of tumor suppressor genes may have therapeutic significance in the treatment of cancer. The TRansgenic Adenocarcinoma of Mouse Prostate (TRAMP) SV40 transgenic model provides an excellent system to study disruption of the DNA methylation process in prostate cancer and to determine whether inhibition of DNMTs abrogates prostate tumorigenesis. I have characterized Dnmt expression, locus specific hypermethylation, and global and repetitive element hypomethylation in the TRAMP model. I have also utilized a Dnmt1 hypomorphic model crossed with the TRAMP model to test the role of Dnmt1 in TRAMP tumor development and progression. The information gained from this study permits a better understanding of aberrant DNA methylation in prostate cancer and how targeting of these alterations may affect prostate cancer progression.

Specific Aims:

1. Identify and characterize the biological significance of genes that have altered DNA methylation status in TRAMP.
2. Determine whether genetic disruption of DNMT1 inhibits prostate tumorigenesis in TRAMP.

Body:

Examination of the Role of DNA Methylation Changes in Prostate Cancer using the Transgenic Adenocarcinoma of Mouse Prostate (TRAMP) Model

Task 1. Identify and characterize the biological significance of genes that have altered DNA methylation status in TRAMP:

The goal of this task was to identify genes that were commonly silenced by promoter hypermethylation in TRAMP tumors and then to determine if these genes had tumor suppressor activity. The first part of this task took much longer than expected to complete thus the second part of this task was not finished. However, several interesting and unexpected observations were made from these studies. Initially, I performed Restriction Landmark Genomic Scanning (RLGS) on several stages and types of TRAMP tumors and compared these to normal prostate samples [1-3]. However, this analysis only resulted in identification of one gene (Irx3) displaying decreased expression and promoter methylation in TRAMP tumors (Table 1, Figure 1) [1-3]. Interestingly, I identified a number of loci that displayed gene body or downstream aberrant DNA methylation correlating with increased expression, including p19 and p16, which are encoded in the Cdkn2a locus (Table 1, Figure 2) [1-3]. Next I attempted to identify promoter methylated, silenced genes by a candidate approach, wherein I examined the expression and methylation of several genes in TRAMP tumors that have been shown to display this pattern in human prostate cancer. Interestingly, several of these candidate genes, including the Gst genes, Mgmt, Pdlim4, and Zfp185, did display reduced expression in TRAMP tumors, but were not methylated in their promoter regions (Figure 3) [4]. Pharmacological inhibition of Dnmts and Hdacs suggested that epigenetic mechanisms besides DNA methylation may play a role in the regulation of the Gst genes (Figure 4) [4].

As a final approach, I utilized a microarray based technique, HpaII Tiny Fragment Enrichment by Ligation-Mediated PCR (HELP), to identify genes that display aberrant promoter methylation in TRAMP tumors. The array that is used for this assay is a Nimblegen tiling array, designed by Dr. John Greally at the Albert Einstein School of Medicine, which covers the entire mouse genome. I have completed HELP analysis on both normal mouse prostate and TRAMP tumor samples, which reveal many aberrant hypermethylation and hypomethylation events in TRAMP as compared to normal prostate (Figure 5). From this I identified a list of genes that display promoter hypermethylation in TRAMP tumors, indicating that these genes are silenced because they have tumor suppressive activities (Table 2) [5]. In addition, this analysis allowed me to identify genes that are hypomethylated in their promoter regions in TRAMP tumors, suggesting that they may be expressed in prostate cancer and have oncogenic functions (Table 2). The known functions of these hypermethylated genes ranges from protein phosphorylation and chromatin regulation to transcription and translation. Interestingly, one of the most highly methylated genes in TRAMP, Elac2, has been shown to be associated with prostate cancer incidence (Table 2). Furthermore, Elac2 is known to interact with Smad2, Fast-1, and Tgf-beta and reduced expression of Elac2 has been shown to inhibit Tgf-beta induced growth arrest [6]. My data suggest that DNA methylation is a mechanism for the regulation of this gene in TRAMP. Future studies will be required to fully determine the regulation of these genes in prostate cancer and their roles in inhibiting or promoting prostate cancer progression.

Task 2. Determine whether genetic disruption of DNA methyltransferase 1 (DNMT1) inhibits prostate tumorigenesis in TRAMP:

The prostates of Dnmt1 hypomorphic mice have not been characterized previously. Therefore, the first goal of this task was to determine whether Dnmt1 hypomorphic mice have normal prostate development. These mice can have four possible genotypes, WT, R/+, N/+, and N/R and previously it had been shown that the heterozygous mice have approximately 50% of normal Dnmt1 expression whereas N/R mice have only 10% of normal Dnmt1 expression. I find that *Dnmt1* mRNA expression is reduced in prostate tissue from the different genotypes of Dnmt1 hypomorphic mice as expected (Figure 6A). In contrast, *Dnmt3a* and *Dnmt3b* displayed variable expression patterns, with no clear change in the prostate of Dnmt hypomorphic mice (Figure 6A). I also measured global DNA methylation as determined by total 5-methyl-deoxycytidine (5mdC) levels and methylation of the B1 repetitive element. As expected, based on a previous study of centromeric repeat methylation in these mice [7], there was a significant decrease in global and repetitive element methylation in prostates and livers from N/R mice as compared to the WT mice, while significant hypomethylation was not observed in R/+ or N/+ mice (Figure 6B).

Next, I sacrificed Dnmt1 hypomorphic mice at 15 and 24 weeks of age and measured prostate weight, performed gross anatomical dissections of the prostates, examined glandular morphology with hematoxylin and eosin (H&E) staining, and examined the expression of several prostate specific differentiation markers using Immunohistochemistry (IHC). No survival defects in Dnmt1 hypomorphic mice had previously been reported [7]. However, as compared to WT, R/+, and N/+ mice, I found that there were only 20% of the expected Mendelian Ratio of N/R mice (Table 3). In contrast, R/+ and N/+ mice were generated at the expected levels (Table 3). I also found that N/R mice had decreased body weight at 15 and 24 weeks, and reduced prostate weight at 15 weeks of age (Figure 7A & B). However, after normalization to body weight, the prostate weights of these mice were not significantly different amongst the four genotypes (Figure 7C). These data indicate that N/R mice have a general survival and size defect but that it does not specifically affect the prostate. Finally, I performed H&E staining and IHC analyses of several prostate differentiation markers on embedded prostate tissue from Dnmt1 hypomorphic mice. The markers examined include p63 (basal cells), smooth muscle actin, AR (androgen receptor), and e-cadherin (luminal cells). Thorough examination of tissues from the four different genotypes revealed normal glandular morphology and cell differentiation marker expression (Figure 8A & B), suggesting that the prostates of Dnmt1 hypomorphic mice develop normally. In addition, R/+, N/+, and N/R mice are fertile. Taken together, these data indicate that the prostates of Dnmt1 hypomorphic mice develop normally and are functional.

The second goal of this task was to generate TRAMP DNMT1 hypomorphic mice. The Dnmt1 hypomorphic mice are in a pure C57Bl/6 background [7]. In the above described studies of DNA methylation in TRAMP I utilized 50:50 C57Bl/6:FVB strain TRAMP mice as they typically present with tumors that are contained within the prostate rather than spreading to the seminal vesicles [1-3]. To generate Dnmt1 hypomorphic TRAMP mice in the 50:50 strain background, it was necessary to backcross mice carrying the Dnmt1 hypomorphic alleles to a FVB TRAMP strain homozygous for the TRAMP transgene. I established and maintained colonies of R/+ and N/+ mice that have been backcrossed to FVB TRAMP four times. These mice are 93.75% FVB, and when crossed to C57Bl/6 they produce f1 mice which are 46.9% FVB:53.1% C57Bl/6, approximating a 50:50 genetic ratio. All of the final mice used in this study were generated by crossing F4 R/+ TRAMP FVB mice with N/+ C57Bl/6 mice. To best overcome differences in tumor pathology due to strain, I compared only age matched littermates of the four possible Dnmt1 hypomorphic genotypes (+/+, N/+, R/+, N/R). We

collected samples from approximately 20 animals per genotype for each time point. At the early time points (12 and 15 weeks of age) prostate tissue from half of the mice was embedded for histological analysis and prostate tissue from the other half was frozen for molecular analysis, due to the limited size of the prostate at this age. At the later time point (24 weeks), prostate tissue was first embedded and the remaining tissue was frozen for molecular analyses.

To confirm specific knockdown of Dnmt1, I measured Dnmt1, Dnmt3a, and Dnmt3b mRNA and protein expressions in the prostates of TRAMP Dnmt1 hypomorphic mice. *Dnmt1* mRNA expression is decreased in hypomorphic mouse prostates, particularly in N/R mice, at all three time points (Figure 9A). In contrast, *Dnmt3a* and *Dnmt3b* mRNA expression shows variability amongst the four genotypes, with the only significant change being an increase in *Dnmt3a* in prostate tissue from TRAMP N/+ mice at 24 weeks of age (Figure 9B & C). Similar to *Dnmt1* mRNA expression, Dnmt1 protein levels were decreased in hypomorphic mice as shown by Western blot analysis (Figure 10A & B). IHC staining for Dnmt1 in prostate tissue from 24 week old TRAMP Dnmt1 hypomorphic mice also revealed dramatically lower Dnmt1 protein levels in TRAMP N/R mice compared to TRAMP +/+ mice (Figure 11). Dnmt3a and Dnmt3b protein levels were more variable, but tended to have higher average expression levels in Dnmt1 hypomorphic mice, with significant increases in Dnmt3b in 15 week old TRAMP R/+ mice and 24 week old TRAMP N/+ mice (Figure 10C & D). Together these data show that Dnmt1 expression is substantially decreased in TRAMP Dnmt1 hypomorphic mouse prostates and that Dnmt3a and Dnmt3b expressions are increased sporadically, suggesting a compensatory mechanism for reduced Dnmt1 expression in the TRAMP prostate.

To determine whether decreased Dnmt1 expression affected genomic DNA methylation, I measured 5mdC levels and B1 repetitive element methylation levels in prostate and liver tissues from TRAMP Dnmt1 hypomorphic mice. 5mdC levels are decreased in TRAMP N/R mouse prostates at all ages and TRAMP N/+ mouse prostates at 15 and 24 weeks of age (Figure 12A-C). B1 methylation levels are unchanged at 12 weeks but are decreased at 15 and 24 weeks in TRAMP N/R mice and at 15 weeks of age in TRAMP N/+ mice (Figure 12D-F). Overall, these data confirmed the expected DNA methylation phenotypes of Dnmt1 hypomorphic mice. I next tested whether reduced Dnmt1 expression prevented aberrant locus-specific hypermethylation in TRAMP tumors. I performed MAQMA analysis on prostate samples from 24 week old TRAMP Dnmt1 hypomorphic mice for four loci we had previously identified to be commonly hypermethylated in late stage TRAMP tumors [1-3]. Irx3 displays promoter hypermethylation while Cacna1a, Cdkn2a, and Nrxn2 display downstream gene hypermethylation in TRAMP [1-3]. Notably, we observed a decrease in DNA methylation of the Irx3 gene promoter in Dnmt1 hypomorphic TRAMP mice compared to TRAMP +/+ mice, with significant decreases in TRAMP N/+ and TRAMP N/R mice (Figure 13A). In contrast, we observed no consistent methylation change at Cacna1a, Cdkn2a, and Nrxn2 in the TRAMP Dnmt1 hypomorphic mice compared to TRAMP +/+ mice, with one significant decrease in TRAMP R/+ mice at the Nrxn2 locus (Figure 13B-D). Finally, we performed HELP analysis on several TRAMP Dnmt1 hypomorph tumor samples. From this we identified several genes that were hypomethylated in TRAMP N/R prostate tissue as compared to TRAMP +/+ prostate tissue (Table 4). Furthermore, comparison of the percent hypomethylation of gene bodies versus gene promoters revealed that there was more hypomethylation of promoter regions than downstream regions at 24 weeks of age in TRAMP Dnmt1 hypomorph tumors (Table 5). These data suggest that Dnmt1 may play a more prominent role in establishing or maintaining tumor-specific promoter hypermethylation than aberrant downstream hypermethylation.

The final goal of this task was to determine whether tumor progression was altered in TRAMP Dnmt1 hypomorphic mice. I measured several parameters in TRAMP Dnmt1 hypomorphic mice, including body and prostate weight, primary tumor incidence, palpable tumor incidence, and metastatic tumor incidence. At 12 and 15 weeks of age, there was no change in prostate weight, after normalization by body weight, in Dnmt1 hypomorphic mice, except a slight but significant increase in N/R mice at 15 weeks (Figure 14A). Conversely, prostate weights are decreased in TRAMP R/+ and TRAMP N/R mice compared to TRAMP +/+ mice at 24 weeks of age (Figure 14A). These data provided initial indication that reduced Dnmt1 expression may have opposing effects on prostate cancer progression depending on the tumor stage/time point analyzed. Primary tumor incidence data also were consistent with this idea. At 12 and 15 weeks of age Dnmt1 hypomorphic mice displayed increased primary tumor incidence compared to WT TRAMP mice, with almost twice as many animals presenting with primary tumors in TRAMP N/+ mice as compared to TRAMP +/+ mice (Figure 14B; Table 6). In contrast, at 24 weeks of age, WT and Dnmt1 hypomorphic mice have similar primary tumor incidence. Moreover, R/+ and N/R mice showed reduced incidence of palpable tumors at 24 weeks (Figure 14B; Table 6).

To further assess the effect of hypomorphic Dnmt1 expression on tumorigenesis in the TRAMP model, examined metastatic tumor growth. As expected, roughly one-third of TRAMP +/+ mice developed lymph node or distant site metastases at 24 weeks of age (Figure 15C; Table 6). Strikingly, the incidence of macro-metastases was greatly reduced in all strains of Dnmt1 hypomorphic mice, with complete elimination of metastases in N/R mice (Figure 16C; Table 6). To assess micro-metastatic incidence in TRAMP Dnmt1 hypomorphic mice, I performed IHC staining for SV40 T antigen (Tag) on lymph node, liver, lung, and kidney tissues, common sites of metastases in TRAMP [8,9]. This allowed me to identify microscopic metastases not visible at necropsy. Interestingly, I found that TRAMP R/+ and TRAMP N/+ mice displayed similar levels of microscopic metastases at both local (draining lymph nodes) and distant organs (kidney, lung, liver) as compared to TRAMP +/+ mice (Table 7). However, while TRAMP N/R mice showed Tag positive staining in the draining lymph nodes of the prostate, no micro-metastases were observed in any distant organs of these mice (Table 7). These data indicate that the early steps of metastasis, such as intravasation, are not prevented in TRAMP N/R mice, but later steps of metastasis, such as extravasation or colonization, are inhibited.

I next measured the stage of primary tumor progression microscopically by examining H&E stained prostate tissues. Tissue sections were scored for tumor stage (Normal-N, Prostatic Intraepithelial Neoplasia-PIN, Well Differentiated-WD, Moderately Differentiated-MD, and Poorly Differentiated-PD) and the percent of tissue observed of each pathological stage was determined as described previously [9]. To compare the pathological state between TRAMP genotypes, I calculated a Disease Index (DI) based on the percent of each pathological stage determined for each prostatic lobe. Because TRAMP mice normally develop tumors in the dorsal, lateral, and ventral lobes, I combined the percent pathological stage and DI values for these three lobes in each genotype. This analysis revealed that 12 week old TRAMP N/R mice have increased tumor progression compared to TRAMP +/+ mice (Fig. 17A). Additionally, both TRAMP N/+ and TRAMP N/R mice display significantly increased progression state at 15 weeks compared to TRAMP +/+ mice (Fig. 17B). Conversely, both TRAMP R/+ and TRAMP N/R mice have significantly *decreased* DI values compared to TRAMP +/+ mice at 24 weeks of age (Fig. 17C). Overall, these data provide further evidence that Dnmt1 has tumor suppressive activity during the early stages and oncogenic function during the later stages of tumor progression in TRAMP mice.

Key Research Accomplishments:

Key Scientific Findings:

Task 1:

- Restriction Landmark Genomic Scanning (RLGS) analysis of methylation patterns in TRAMP revealed a small number of hypermethylation events in PIN and WD lesions, with a great increase in PD and LS tumors.
- LPD, AIP and MET tumor phenotypes each display numerous hypermethylation events, with the most homogeneous hypermethylation pattern in AIP tumors and the most heterogeneous hypermethylation pattern in metastases.
- There are several loci that displayed a tumor phenotype specific methylation status, suggesting that selection may play a role in the development of these patterns.
- Hypermethylated genes revealed by RLGS showed hypermethylation of downstream exons correlating with mRNA overexpression.
- BC058385, Goosecoid (GSC), p19/ARF, p16INK4a, NRXN2 and Cacna1a display downstream hypermethylation correlating with robust mRNA overexpression.
- Overexpression of *p16, p19,* and *Cacna1a* but not downstream hypermethylation, occurs in early stage prostatic lesions in TRAMP, suggesting that gene overexpression is the initiating event.
- Pharmacological reversal of downstream gene hypermethylation in TRAMP cell lines led to decreased expression of *p19* and *p16*, suggesting that downstream hypermethylation contributes to the maintenance of increased gene expression.
- There are several genes (Mgmt, Pdlim4, Zfp185, and Glutathione-s-transferases) that are commonly hypermethylated in human prostate cancer that are also downregulated at the transcriptional level in TRAMP tumors. In TRAMP these genes are not regulated by DNA methylation, but perhaps some other epigenetic mechanism.
- HELP analysis revealed a number of promoter hypermethylated genes in TRAMP tumors as compared to normal prostate. One such gene, Elac2, may be important for prostate cancer incidence.

Task 2:

Dnmt1 hypomorphic mice:

- N/R mice have significantly decreased *Dnmt1* expression and hypomethylation in prostate tissues compared to WT mice
- N/R Dnmt1 Hypomorphic genotype is not inherited in Mendelian fashion
- N/R mice are smaller in size and prostate weights are similar to WT mice once normalized by body weight
- Histological analysis of prostate tissue for Dnmt1 hypomorphic mice reveals normal glandular morphology

TRAMP Dnmt1 hypomorphic mice:

R/+ TRAMP mice compared to WT TRAMP mice display:

- significantly decreased Dnmt1 mRNA expression only at 24 weeks, with no change in Dnmt3a or Dnmt3b mRNA expression at any timepoint
- significantly decreased Dnmt1 protein expression only at 24 weeks of age, with an increase in Dnmt3b expression at 15 weeks
- no change in B1 methylation or in 5mdC levels at any time point
- slight increases in prostate weight and pathological stage at 15 weeks of age

        - slight decreases in primary tumor and metastatic incidence, as well as decreased pathological stage at 24 weeks
- N/+ TRAMP mice compared to WT TRAMP mice display:
    - only Dnmt1 mRNA or protein expression is decreased at any time point, and increased Dnmt3b protein expression at 24 weeks
    - significantly decreased B1 methylation and 5mdC levels at 15 and 24 weeks of age
    - no significant change in prostate weight at any timepoint
    - increased tumor incidence and pathological stage at 15 weeks of age
    - no change in primary tumor incidence and pathological stage, with slightly decreased metastatic incidence at 24 weeks of age
- N/R TRAMP mice compared to WT TRAMP mice display:
    - significantly decreased Dnmt1 mRNA and protein expression at all timepoints
    - no significant change in Dnmt3A and Dnmt3B mRNA or protein expression at any timepoint
    - significantly decreased 5mdC levels at all time points
    - significantly decreased B1 methylation at 15 and 24 weeks of age
    - increased pathological stage at 12 and 15 weeks of age
    - no change in primary tumor incidence, but slightly decreased pathological stage, and no obvious metastases at necropsy

Resources:

- Gene list of commonly hypermethylated loci in TRAMP from RLGS and HELP analysis
- Dnmt1 hypomorphic mouse colony (C57Bl/6)
- Dnmt1 hypomorphic TRAMP mouse colony (FVB)

Reportable Outcomes:

Manuscripts

1. **Morey Kinney, Shannon R.**, Petra Link, Marien Pascual, John M. Greally, Bryan Gillard, Ellen Karasik, Michael T. Moser, Barbara A. Foster, and Adam R. Karpf. The effects of genetic reduction of Dnmt1 on normal murine prostate development and TRAMP tumor progression. In Preparation.

2. **Morey Kinney, Shannon R.**, Wa Zhang, Bryan Gillard, Ellen Karasik, Michael T. Moser, Barbara A. Foster, and Adam R. Karpf. Lack of evidence for green tea polyphenols as a DNA methylation inhibitor in mice. *Cancer Prevention Research*. December 2009. In Press.

3. Mavis, Cory, **Shannon R. Morey Kinney**, Barbara A. Foster, Adam R. Karpf. Expression level and DNA methylation status of Glutathione-S-transferase genes in normal murine prostate and TRAMP tumors. *TheProstate*. 2009 Sep 1;69(12):1312-24.

4. **Morey Kinney, Shannon R.**, Dominic J. Smiraglia, Smitha R. James, Michael T. Moser, Barbara A. Foster, and Adam R. Karpf. Stage-specific alterations of Dnmt expression, DNA hyper-methylation, and DNA hypomethylation during prostate cancer progression in the TRAMP model. *Molecular Cancer Res*. 6(8) August 2008. Selected as Online First Publication.

5. Camoriano, Marta *****, **Morey Kinney, Shannon R.** *, Michael T. Moser, Barbara A. Foster, James L. Mohler, Donald L. Trump, Adam R. Karpf, and Dominic J. Smiraglia. Phenotype-specific CpG Island Methylation Events in a Murine Model of Prostate Cancer. *Cancer Research* 68, 4173-4182, June 1, 2008.
*Equal contribution

6. **Morey, Shannon R.**, Dominic J. Smiraglia, Smitha R. James, Jihnhee Yu, Michael T. Moser, Barbara A. Foster, and Adam R. Karpf. DNA Methylation Pathway Alterations in an Autochthonous Murine Model of ProstateCancer. *Cancer Research* 66, 11659-11667, December 15, 2006.

Oral Presentations

A. International Meetings

1. **Shannon R. Morey Kinney,** Bryan Gillard, Ellen Karasik, Michael T. Moser, Barbara A. Foster, and Adam R.Karpf. The effects of genetic reduction of Dnmt1 on normal prostate development and prostate tumorigenesis in the TRAMP model. 100th Annual AACR Annual Meeting, Denver, CO, April, 2009.

2. **Shannon R. Morey**, Dominic J. Smiraglia, Smitha R. James, Jihnhee Yu, Michael T. Moser, Barbara A. Foster and Adam R. Karpf. Epigenetic Deregulation in a Mouse Model of Prostate Cancer. 97th Annual AACR Meeting, Washington D.C., April, 2006.

B. Regional Meetings

1. **Shannon R. Morey Kinney**. The Effects of Genetic Reduction of Dnmt1 on TRAMP tumor progression and metastasis. Pharmacology and Therapeutics Departmental Retreat, Holiday Valley Resort and Conference Center, Ellicottville, NY, October 2008.

2. **Shannon R. Morey Kinney**, Dominic J. Smiraglia, Smitha R. James, Michael T. Moser, Barbara A. Foster, and Adam R. Karpf. Stage specific alterations of the DNA methylation pathway in a mouse model of prostate cancer. DNA Function Meeting, Roswell Park Cancer Institute, March, 2008

3. **Shannon R. Morey**, Dominic J. Smiraglia, Barbara A. Foster, and Adam R. Karpf. Alterations in DNA Methylation During TRAMP Tumor Progression. Annual Pharmacology Sciences Day, University at Buffalo, May, 2007.

4. **Shannon R. Morey**. Cancer Epigenetics as Seen Through the Eyes of a Mouse. Invited lecture 2007 Science Decade Lecture Series, Roswell Park Cancer Institute, March, 2007

5. **Shannon R. Morey**, Dominic J. Smiraglia, Michael T. Moser, Barbara A. Foster and Adam R. Karpf. Aberrant DNA Hypermethylation is an Early Event During Prostate Tumor Progression in the TRAMP Model. DNA Function Meeting, Roswell Park Cancer Institute, November, 2006

6. **Shannon R. Morey**, Dominic J. Smiraglia, Smitha R. James, Jihnhee Yu, Michael T. Moser, Barbara A. Foster, and Adam R. Karpf. Epigenetic Deregulation in a Mouse Model of Prostate Cancer. Annual Pharmacology Sciences Day, University at Buffalo, May, 2006.

7. **Shannon R. Morey**, Dominic J. Smiraglia, Smitha R. James, Jihnhee Yu, Michael T. Moser, Barbara A. Foster and Adam R. Karpf. Aberrant DNA Hypermethylation in the TRansgenic Adenocarcinoma of Mouse Prostate (TRAMP). DNA Function Meeting, Roswell Park Cancer Institute, March, 2005

Poster Presentations

A. International Meetings

1. **Shannon R. Morey Kinney**, Dominic J. Smiraglia, Smitha R. James, Michael T. Moser, Barbara A. Foster, and Adam R. Karpf. Stage-specific alterations of Dnmt expression, DNA hyper-methylation, and DNA hypomethylation during prostate cancer progression in the TRAMP model. AACR Cancer Epigenetics Meeting, Boston, MA, May, 2008.

2. **Shannon R. Morey Kinney**, Marta Camoriano, Michael T. Moser, Barbara A. Foster, Dominic J. Smiraglia, and Adam R. Karpf. Restriction Landmark Genomic Scanning Reveals Phenotype Specific Epigenomic Patterns in a Mouse Model of Prostate Cancer. Keystone Cancer Genomics and Epigenomics Symposium, Taos, NM, February, 2008.

3. **Shannon R. Morey**, Dominic J. Smiraglia, Michael T. Moser, Barbara A. Foster, and Adam R. Karpf. DNA Methylation Pathway Alterations in a Mouse Model of Prostate Cancer. AACR Edward A. Smuckler Memorial Pathobiology of Cancer Workshop, Snowmass, CO, July, 2007.

4. **Shannon R. Morey**, Dominic J. Smiraglia, Michael T. Moser, Barbara A. Foster and Adam R. Karpf. Aberrant DNA Hypermethylation is an Early Event During Prostate Tumor Progression in the TRAMP Model. Innovations in Prostate Cancer Research AACR Meeting, San Francisco CA, December, 2006

5. **Shannon R. Morey**, Dominic J. Smiraglia, Smitha R. James, Jihnhee Yu, Michael T. Moser, Barbara A. Foster, and Adam R. Karpf. Epigenetic Deregulation in a Mouse Model of Prostate Cancer. CSHL Mechanisms & Models of Cancer Meeting, Cold Spring Harbor, NY August, 2006.

B. Regional Meetings

1. **Shannon R. Morey Kinney**, Marta Camoriano, Michael T. Moser, Barbara A. Foster, Dominic J. Smiraglia, and Adam R. Karpf. Restriction Landmark Genomic Scanning Reveals Phenotype Specific Epigenomic Patterns in a Mouse Model of Prostate Cancer. Annual Pharmacology Sciences Day, University at Buffalo, May, 2008.

2. **Shannon R. Morey Kinney**, Dominic J. Smiraglia, Michael T. Moser, Barbara A. Foster, and Adam R. Karpf. Comparison of Altered DNA Methylation During Prostate Cancer Progression Using the TRAMP Model. 14th Annual Thanksgiving Poster Forum. Roswell Park Cancer Institute, Buffalo, NY, November, 2007.

3. **Shannon R. Morey Kinney**, Dominic J. Smiraglia, Michael T. Moser, Barbara A. Foster, and Adam R. Karpf. Comparison of Altered DNA Methylation During Prostate Cancer Progression Using the TRAMP Model. Pharmacology and Therepeutics Departmental Retreat, Holiday Valley Resort and Conference Center, Ellicottville, NY, November, 2007.

4. **Shannon R. Morey**, Dominic J. Smiraglia, Smitha R. James, Jihnhee Yu, Michael T. Moser, Barbara A. Foster, and Adam R. Karpf. Epigenetic Deregulation in a Mouse Model of Prostate Cancer. Annual Sigma Xi Student Research Competition, University at Buffalo, April, 2006.

6. **Shannon R. Morey**, Dominic J. Smiraglia, Smitha R. James, Jennifer Jackson, Angela Szafranek, Michael Moser, Barbara A. Foster and Adam R. Karpf. Aberrant DNA Methylation in the TRansgenic Adenocarcinoma of Mouse Prostate. Annual Pharmacology Sciences Day, University at Buffalo, May, 2005

Awards

2009 AACR-Aflac, Inc. Scholar-in-Training Award to attend the AACR 100th Annual Meeting
2007 Selected for AACR Edward A. Smuckler Memorial Pathobiology of Cancer Workshop
2006 Best Poster Award, University at Buffalo Sigma Xi Student Research Competition

Conclusions:

Although the original goals of Specific Aim 1 were not completed, several novel and important observations were made from these studies. For instance, the phenomenon of cancer specific gene body methylation correlating with overexpression of those genes had rarely been reported, and had only been reported for the CDKN2A locus in human prostate cancer [10]. Interestingly, this was the most common gene body hypermethylation event in TRAMP tumors [1-3]. In addition, we identified several genes, including the Gst family of genes, that are downregulated in TRAMP tumors as compared to normal prostate that may be regulated by an epigenetic mechanism besides DNA methylation. This supports the use of the TRAMP model to study prostate cancer as these genes are also commonly silenced in human prostate cancer. Finally, HELP analysis confirmed that promoter specific hypermethylation and hypomethylation occur during TRAMP tumor development.

The three main goals of Specific Aim 2 were to characterize the prostate development in Dnmt1 hypomorphic mice, determine if TRAMP Dnmt1 hypomorphic mice have altered tumor progression, and characterize the DNA methylation changes that occurred in TRAMP Dnmt1 hypomorphic tumors. N/R mice had a significant survival defect, as well as reduced body weight. Furthermore, hypomorphic Dnmt1 expression caused DNA hypomethylation in the prostate but general prostate architecture and differentiation state appeared normal. Dnmt expression data suggest that Dnmt3a and Dnmt3b expression are retained or increased following Dnmt1 reduction, providing a potential compensatory mechanism for survival and tissue development.

My initial studies in TRAMP mice revealed that global and repetitive element hypomethylation occur early during the development of prostate cancer in TRAMP while locus specific DNA hypermethylation occurs late during TRAMP tumor development [3]. Based on based on this, we hypothesized that Dnmt1 could play a dual role in CaP whereby it has tumor suppressor activity during early stages of the disease and oncogenic function at late stages of the disease. I found that further DNA hypomethylation in TRAMP caused by expression of hypomorphic Dnmt1 alleles resulted in increased tumor incidence and significantly accelerated disease progression at both 12 and 15 weeks of age. Global DNA hypomethylation is known to be associated with both genomic instability and oncogene expression, both of which contribute to oncogenesis [11,12]. This suggests that these mechanisms could also be operative in the TRAMP model, and demonstrate that DNA hypomethylation promotes the initial stages of prostate cancer progression. In addition, examination of tumor progression at 24 weeks of age revealed that reduced expression of Dnmt1 delays tumorigenesis and inhibits the development of prostate cancer metastases. In agreement with our findings, Day and colleagues have shown that treatment of either intact or castrated TRAMP mice with the DNA methyltransferase inhibitor 5-aza-2'-deoxycytidine (DAC) inhibits both primary tumor growth as well as the development of lymph node metastases [13,14].

Several types of analyses revealed altered DNA methylation in the Dnmt1 hypomorphic mice as compared to WT mice. This was true at a global level as well as at specific loci. Interestingly, it appears that promoter methylation is more reduced in Dnmt1 hypomorphic mice than aberrant gene body methylation. This suggests that Dnmt1 may play a more prominent role in promoter methylation than it does in downstream DNA methylation. My findings from the TRAMP Dnmt1 hypomorphic mouse model suggest that Dnmt1 has opposing effects on early and late stage prostate cancer. Our findings support the use of Dnmt1 inhibitors as therapeutic interventions for late-stage and metastatic prostate cancer, but not as prostate chemoprevention approaches in high-risk patients.

References:

1. Morey SR, Smiraglia DJ, James SR, Yu J, Moser MT, Foster BA, Karpf AR: **DNA methylation pathway alterations in an autochthonous murine model of prostate cancer**. *Cancer Res* 2006, **66**:11659-11667.
2. Camoriano M, Kinney SR, Moser MT, Foster BA, Mohler JL, Trump DL, Karpf AR, Smiraglia DJ: **Phenotype-specific CpG island methylation events in a murine model of prostate cancer**. *Cancer Res* 2008, **68**:4173-4182.
3. Morey Kinney SR, Smiraglia DJ, James SR, Moser MT, Foster BA, Karpf AR: **Stage-specific alterations of DNA methyltransferase expression, DNA hypermethylation, and DNA hypomethylation during prostate cancer progression in the transgenic adenocarcinoma of mouse prostate model**. *Mol Cancer Res* 2008, **6**:1365-1374.
4. Mavis CK, Morey Kinney SR, Foster BA, Karpf AR: **Expression level and DNA methylation status of glutathione-S-transferase genes in normal murine prostate and TRAMP tumors**. *Prostate* 2009, **69**:1312-1324.
5. Morey Kinney SR, Wa Zhang, Marien Pascual, John M. Greally, Bryan M. Gillard, Ellen Karasik, Barbara A. Foster, and Adam R. Karpf: **Lack of Evidence for Green Tea Polyphenols as DNA Methylation Inhibitors in Murine Prostate**. *Cancer Prevention Research* 2009:In Press.
6. Noda D, Itoh S, Watanabe Y, Inamitsu M, Dennler S, Itoh F, Koike S, Danielpour D, ten Dijke P, Kato M: **ELAC2, a putative prostate cancer susceptibility gene product, potentiates TGF-beta/Smad-induced growth arrest of prostate cells**. *Oncogene* 2006, **25**:5591-5600.
7. Eads CA, Nickel AE, Laird PW: **Complete genetic suppression of polyp formation and reduction of CpG-island hypermethylation in Apc(Min/+) Dnmt1-hypomorphic Mice**. *Cancer Res* 2002, **62**:1296-1299.
8. Hurwitz AA, Foster BA, Allison JP, Greenberg NM, Kwon ED: **The TRAMP mouse as a model for prostate cancer**. *Curr Protoc Immunol* 2001, **Chapter 20**:Unit 20 25.
9. Kaplan-Lefko PJ, Chen TM, Ittmann MM, Barrios RJ, Ayala GE, Huss WJ, Maddison LA, Foster BA, Greenberg NM: **Pathobiology of autochthonous prostate cancer in a pre-clinical transgenic mouse model**. *Prostate* 2003, **55**:219-237.
10. Nguyen TT, Nguyen CT, Gonzales FA, Nichols PW, Yu MC, Jones PA: **Analysis of cyclin-dependent kinase inhibitor expression and methylation patterns in human prostate cancers**. *Prostate* 2000, **43**:233-242.
11. Gaudet F, Hodgson JG, Eden A, Jackson-Grusby L, Dausman J, Gray JW, Leonhardt H, Jaenisch R: **Induction of tumors in mice by genomic hypomethylation**. *Science* 2003, **300**:489-492.
12. Eden A, Gaudet F, Waghmare A, Jaenisch R: **Chromosomal instability and tumors promoted by DNA hypomethylation**. *Science* 2003, **300**:455.
13. McCabe MT, Low JA, Daignault S, Imperiale MJ, Wojno KJ, Day ML: **Inhibition of DNA methyltransferase activity prevents tumorigenesis in a mouse model of prostate cancer**. *Cancer Res* 2006, **66**:385-392.
14. Zorn CS, Wojno KJ, McCabe MT, Kuefer R, Gschwend JE, Day ML: **5-aza-2'-deoxycytidine delays androgen-independent disease and improves survival in the transgenic adenocarcinoma of the mouse prostate mouse model of prostate cancer**. *Clin Cancer Res* 2007, **13**:2136-2143.

Appendix

Supporting Data

Table 1. RLGS spots of interest

Spot	PRIM n=30	MET n=30	AIP n=30	Total n=90	Class	[d]P-value	[e]CGI	Context	[g]Gene Homology
3D22	29	23	30	**82**	[a]Frequency		N	3'end	**Cdkn2a**
4C11	21	25	28	**74**	Frequency		N	Body	**4932416N17Rik**
4E25	23	25	26	**74**	Frequency		--	--	**--**
4C38	19	15	28	**62**	Frequency		Y	5' end	**Lhfpl4**
4C31	23	11	25	**59**	Frequency		N	Body	**Adcy5**
4C13	23	9	26	**58**	Frequency		Y	5'end	**AK039621**
3D67	18	17	21	**56**	Frequency		Y	3'end	**Oprd1**
2C28	16	14	22	**52**	Frequency		Y	5'end	**AK004006**
2E04	19	9	13	**41**	Frequency		--	--	**--**
2D21	13	8	15	**36**	Frequency		Y	3'end	**BC025575**
3E56	9	11	15	**35**	Frequency		Y	5' end	**Zfp787**
3E07	7	12	16	**35**	Frequency		Y	5'end	**U2af1-rs1**
6D10	6	12	15	**33**	Frequency		N	Intergenic	**Intergenic**
2C37	11	4	8	**23**	Frequency		Y	5'end	**Hox2.9**
5D52	8	8	5	**21**	Frequency		Y	5'end	**Zar1**
2D39	5	7	6	**18**	Frequency		Y	5'end	**CG869761**
4G73	5	2	3	**10**	Frequency		Y	5'end	**Irx3**
3C21	**20**	1	**27**	48	[b]Prim or AIP	**1.0E-12**	Y	[f]5'end	**Nrxn2**
3E30	**24**	5	**29**	58	Prim or AIP	**2.3E-11**	N	3'end	**Gsc**
5F09	**19**	2	**21**	42	Prim or AIP	**2.5E-08**	N	Body	**Cacna1a**
2G63	**22**	8	**29**	59	Prim or AIP	**7.1E-08**	Y	Body	**BC058385**
2B37	**14**	1	**14**	29	Prim or AIP	**1.0E-05**	--	--	**--**
5B30	**20**	6	**22**	48	Prim or AIP	**1.2E-05**	Y	Body	**AK139829**
4D27	**16**	6	**19**	41	Prim or AIP	**7.0E-04**	Y	5'end	**Hoxa2**
3E16	**8**	0	**8**	16	Prim or AIP	**9.1E-04**	--	--	**--**
4C01	**18**	9	**20**	47	Prim or AIP	**3.0E-03**	Y	5'end	**AK044818**
3D01	**7**	0	**7**	14	Prim or AIP	**3.0E-03**	--	--	**--**
2G10	**8**	0	**6**	14	Prim or AIP	**3.8E-03**	--	--	**--**
2C17	**7**	0	**5**	12	Prim or AIP	**7.0E-03**	--	--	**--**
4C17	**13**	8	**20**	41	Prim or AIP	**1.4E-02**	Y	5' end	**Lhfpl4**
4D69	0	0	**9**	9	[c]AIP specificity	**2.0E-05**	Y	5'end	**Nfyb**
4E04	2	4	**15**	21	AIP specificity	**5.0E-05**	Y	5'end	**Tpm2**
4D54	0	5	**14**	19	AIP specificity	**6.0E-05**	Y	5'end	**Pawr**
4E16	0	1	**9**	10	AIP specificity	**1.0E-04**	Y	5'end	**Tpm2**
3C39	0	0	**7**	7	AIP specificity	**2.0E-04**	Y	5'end	**Mid1ip1**
3G88	5	2	**13**	20	AIP specificity	**1.0E-03**	Y	5'end	**Il6st**

[a]Spots lost in 10 or more samples from all tumor types (n=90); [b]Spots lost significantly in primary tumors plus androgen independent primary tumors (n=60), but not metastatic tumors (n=30); [c]Spots lost significantly in androgen independent primary tumors (n=30), but not in primary plus metastatic tumors (n=60); [d]Fisher's Exact test (two-tailed) for class membership; [e]Is the RLGS spot NotI site within 200bp of a CpG island; [f]Within 5kb of transcriptional start site and/or including exon 1; [g]Annotated gene, mRNA, or spliced EST within 5 kb of the CpG island or NotI site.

Figure 1. Promoter DNA hypermethylation and gene expression in TRAMP.

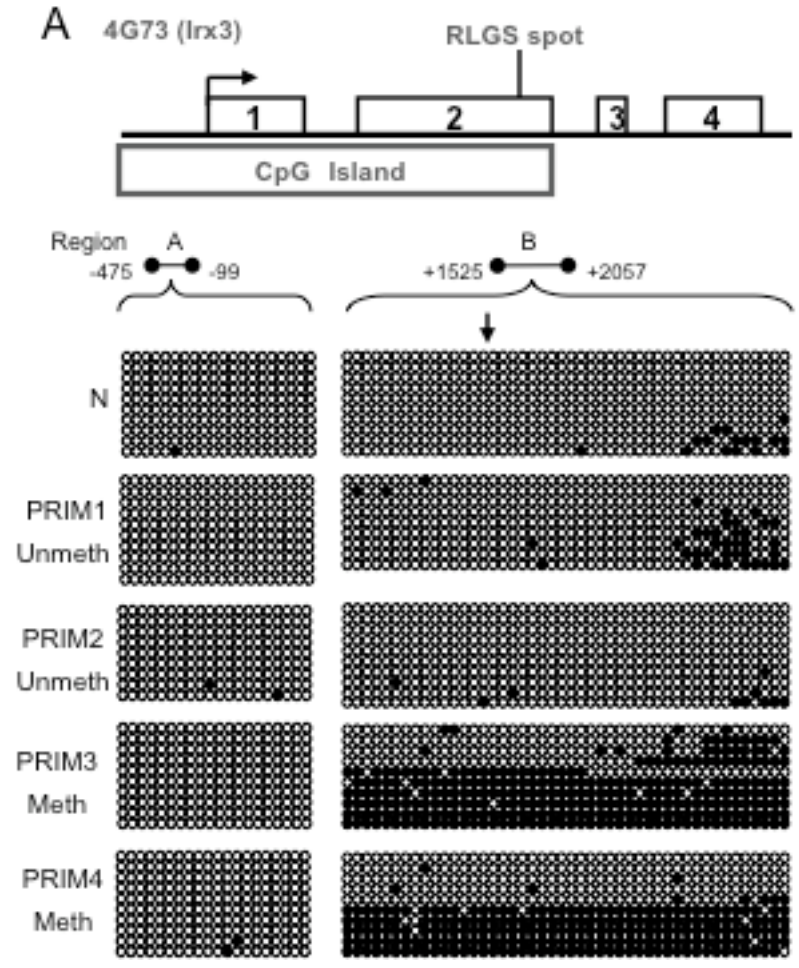

A, Irx3 (RLGS spot 4G73). *Top*, schematic of the *Irx3* gene indicating the regions analyzed by bisulfite sequencing (*horizontal lines bordered by arrows*). *Vertical arrow*, transcriptional start site; *lines*, introns; *boxes*, exons. *Bottom*, bisulfite sequencing of Irx3 of one representative normal prostate, two primary tumors unmethylated by RLGS (PRIM1 and 2), and two primary tumors methylated by RLGS (PRIM3 and 4). *Vertical arrow*, position of the *Not*I site; *rows*, individually sequenced alleles; *open circles*, unmethylated CpG sites; *filled circles*, methylated CpG sites. *B*, *Irx3* mRNA expression in normal prostates and TRAMP primary tumor samples. *Irx3* mRNA expression was measured by qRT-PCR using the C_t method. *Irx3* expression was normalized to *18S rRNA* and is expressed relative to a pooled sample of four strain-matched normal prostates. Expression in 4 normal prostates and 15 primary tumors analyzed by RLGS is indicated. Each symbol indicates a sample and the bar indicates the mean.

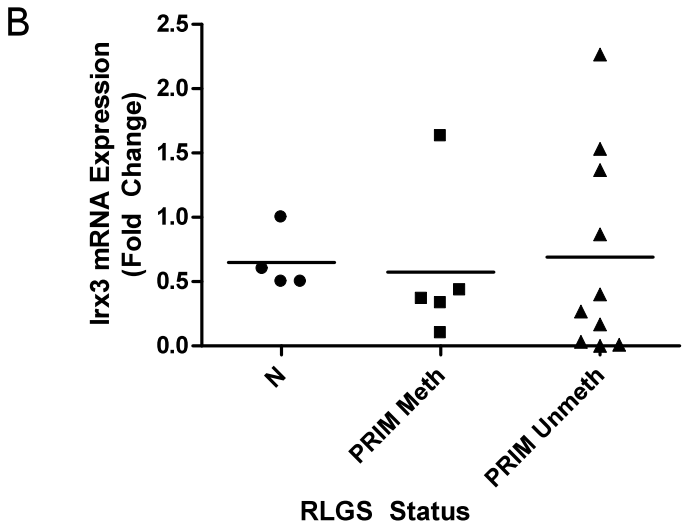

Figure 2. Downstream DNA hypermethylation and gene expression in TRAMP.

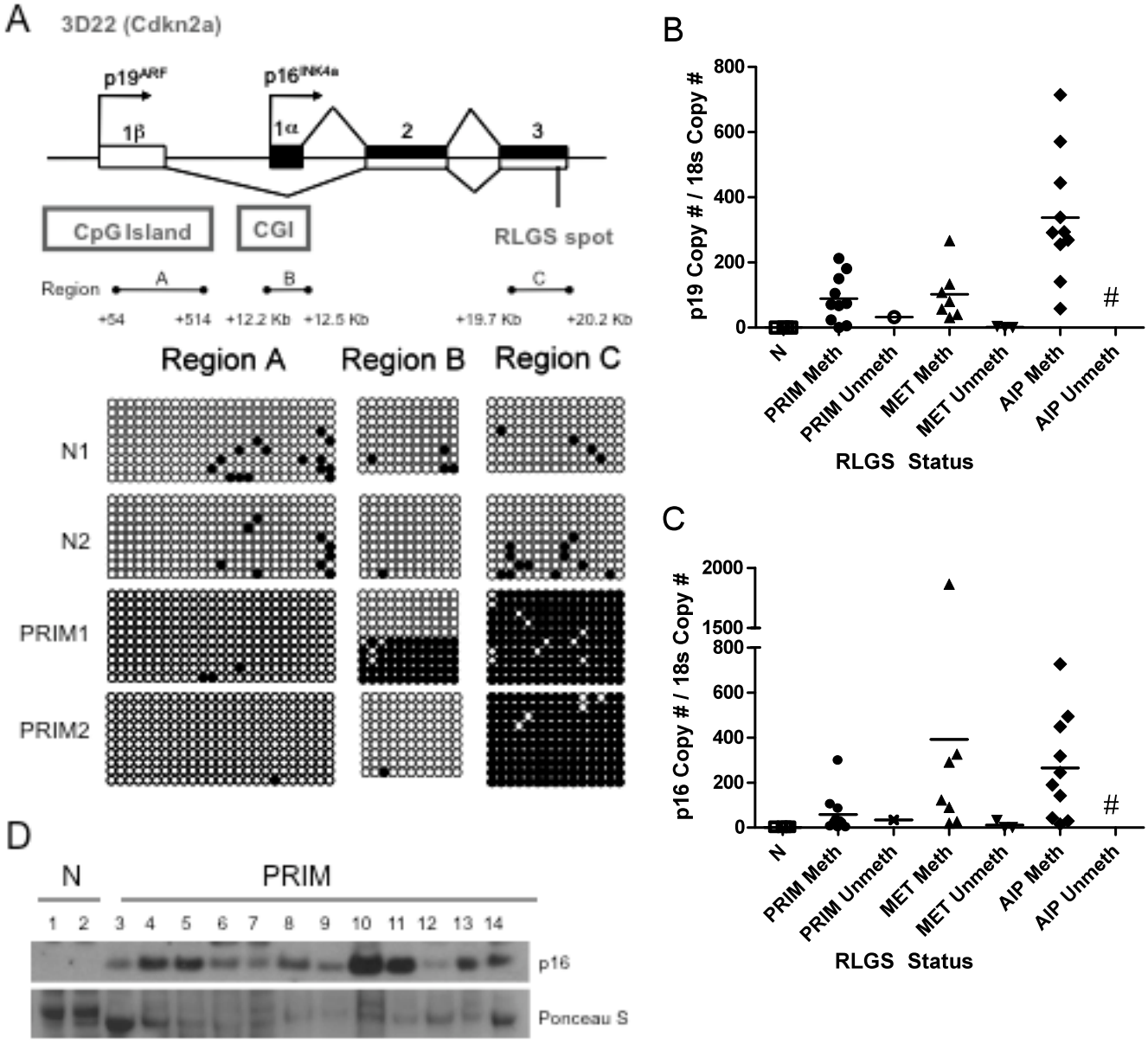

A, methylation analysis of p16 (RLGS spot 3D22). *Top*, schematic of the Cdkn2a locus and the regions analyzed by bisulfite sequencing (*horizontal lines bordered by ovals*). *Bent arrow*, transcriptional start site; *lines*, introns; *boxes*, exons. *Bottom*, sodium bisulfite sequencing of Cdkn2a from two normal prostates and two primary tumors found to be methylated by RLGS. *Vertical arrow*, position of the *Not*I site; *rows*, individually sequenced alleles; *open circles*, unmethylated CpG sites; *filled circles*, methylated CpG sites. *B-C*, *p19* and *p16* mRNA expression in normal prostates and TRAMP tumor samples. Expression was measured by SYBR Green qRT-PCR. Expression was normalized to *18S rRNA*. D, p16 protein expression in normal prostates and TRAMP PRIM tumors. # indicates that there are no samples in this category. p16 protein expression was measured by Western blot analysis of available tumor samples. Ponceau S staining confirmed equivalent protein loading.

Figure 3. Aldh1a2, Mgmt, Pdlim4, and Zfp185 mRNA expression in normal mouse prostate (N) and TRAMP prostate tumors (T).

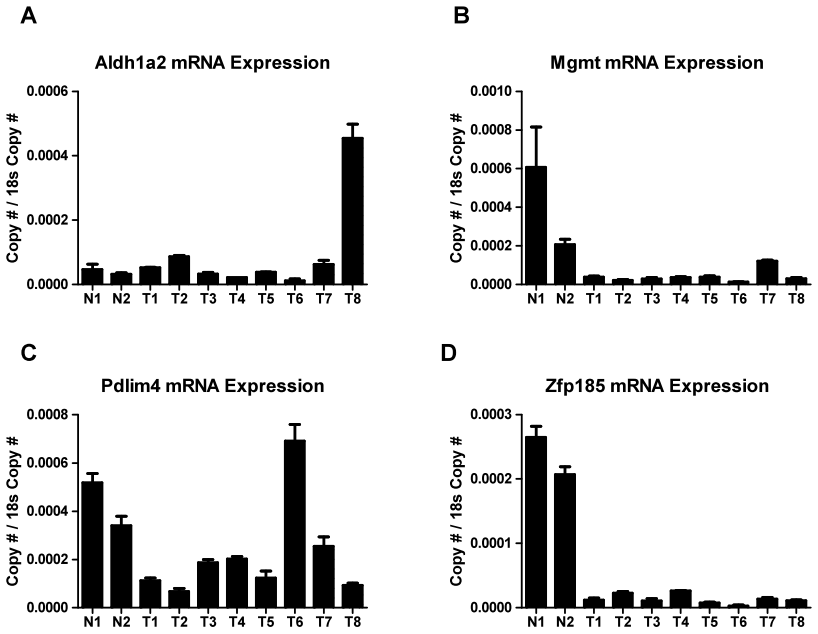

A) Aldh1a2 B) Mgmt C) Pdlim4 D) Zfp185 mRNA levels as determined by SYBR green qRT-PCR. Copy number of target genes were normalized by 18s rRNA endogenous control. E) Mgmt F) Pdlim4 G) Zfp185 promoter methylation status as determined by traditional sodium bisulfite sequencing. Each circle represents a CpG with white circles indicating an unmethylated CpG and black circles indicating a methylated CpG. Each row of circles indicates a separate clone that was sequenced. Bent arrow indicates the transcriptional start site of the gene.

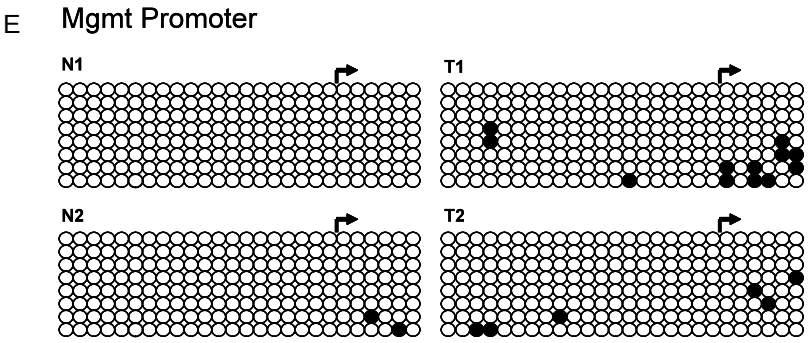

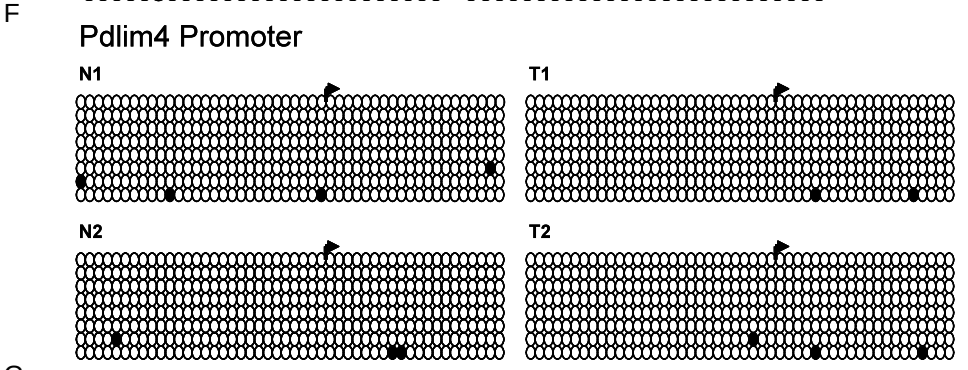

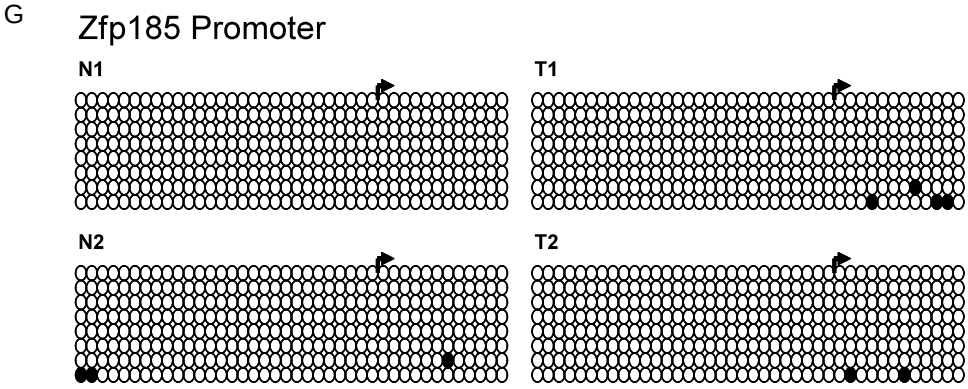

Figure 4. Effect of decitabine and TSA treatment on Gst gene expression in TRAMP-C2 cells.

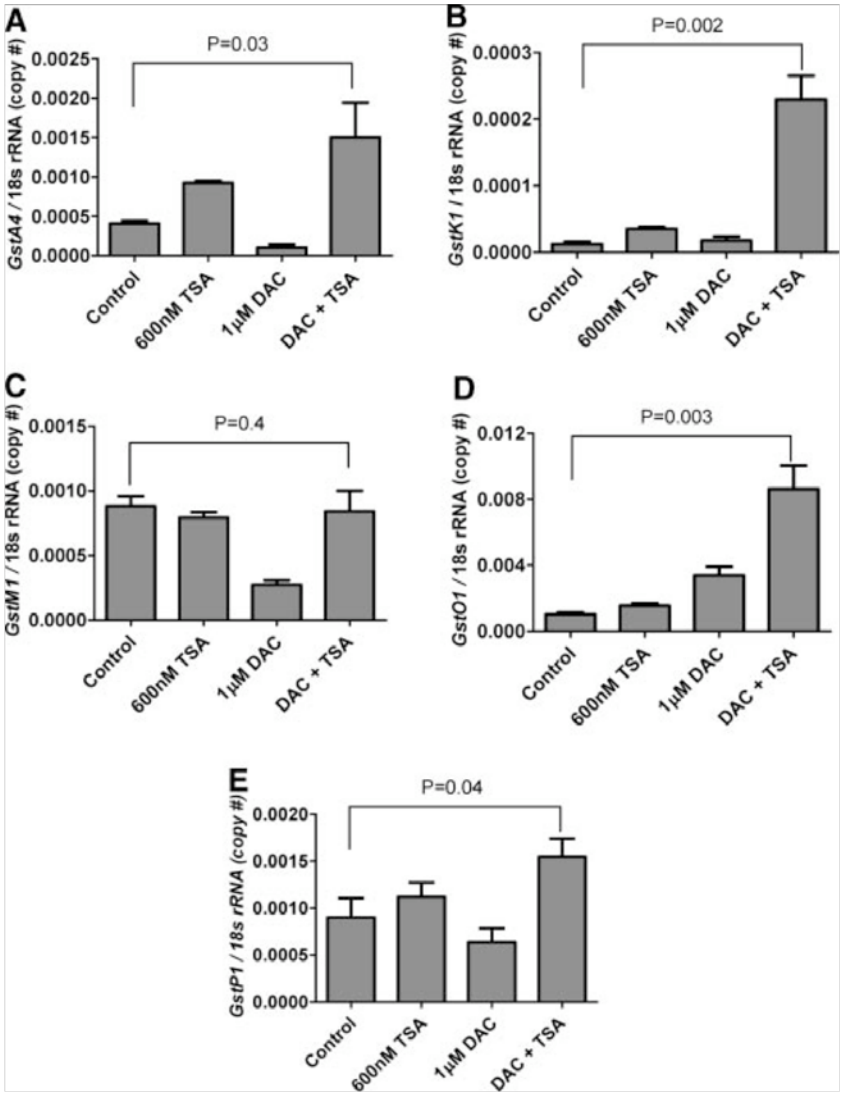

TRAMP-C2 cells were treated with 1.0 mM decitabine (DAC) and/or 600 nM trichostatin A (TSA), and cells were harvest at 5 days post-DAC treatment and/or 1 day post-TSA treatment. The vehicle control consisted of treatment of TRAMP-C2 cells with PBS and DMSO for 5 days and1day, respectively.Gst mRNA expression was measured by qRT-PCR as described in the Materials and Methods Section. A: GstA4, (B) GstK1, (C) GstM1, (D) GstO1, and (E) GstP1. Error bars ¼ SD. Students t-test (unpaired, one-tailed) was performed to test for significant differences in Gst gene expression between control cells and cells treated with DAC and TSA. Results (P-values) are shown on the figure.

Figure 5. Genome wide profiling of green tea treated normal prostate and TRAMP prostate using the HELP assay.

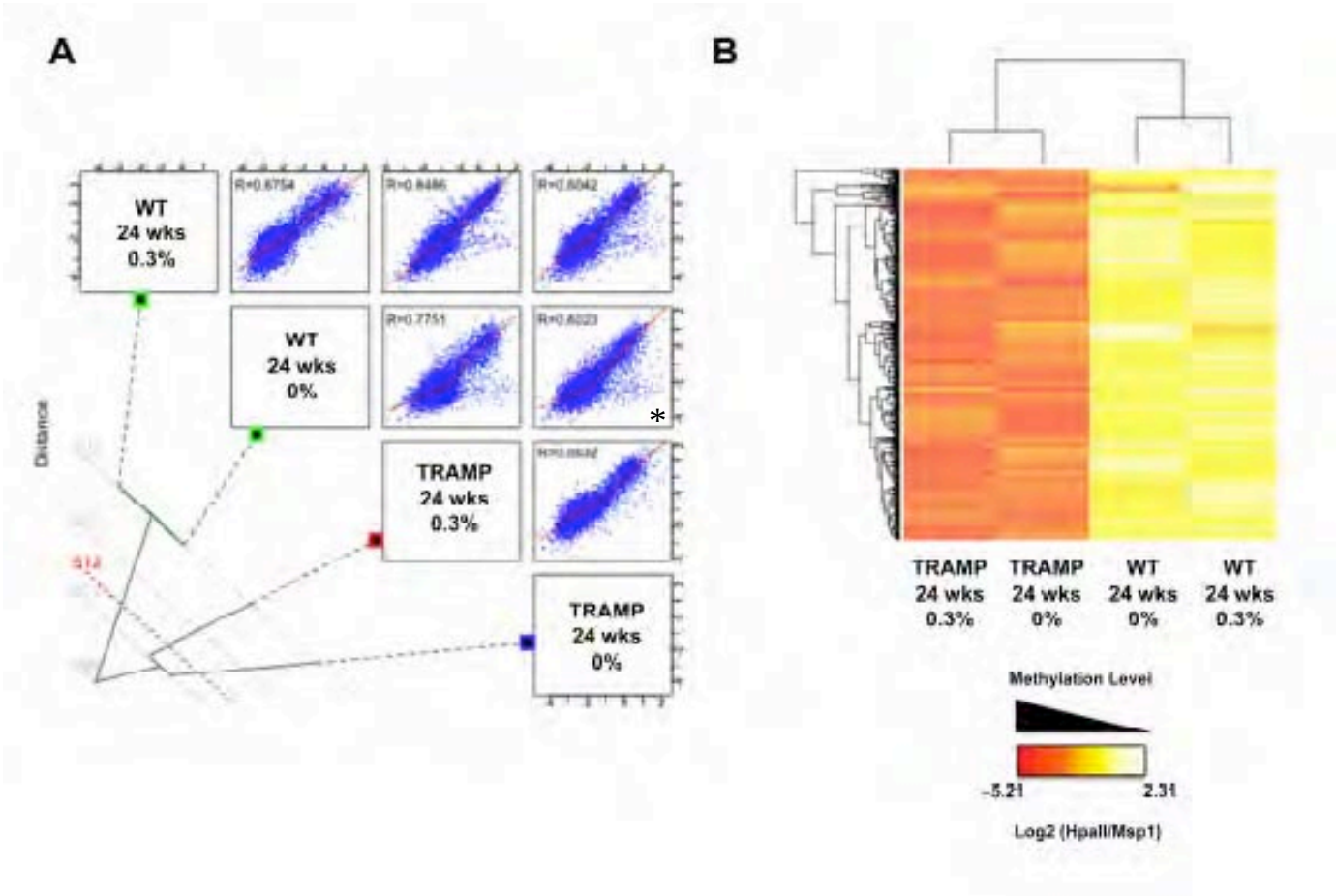

A) Unsupervised clustering of HELP and global pairwise correlations is shown. R values indicate the Pearson correlation for each comparison. The data illustrate the divergence in the methylation pattern in WT versus TRAMP samples. * indicates the direct comparison of untreated WT prostate and TRAMP prostate. Blue dots to the right of the center line indicate hypermethylation events. B) Two-dimensional hierarchical clustering of genes differentially methylated between WT and TRAMP prostate, illustrated by a heatmap. The heat map illustrates 1000 random points selected from this group.

Table 2. Genes displaying significant promoter* hypermethylation or promoter hypomethylation in TRAMP tumor as compared to normal prostate

Hypermethylated Genes				
#	Chromosomal Location	NCBI Gene ID	Strand	Gene Name
1	chr10:60847068-60847202	NM_010124	-	Eif4ebp2
2	chr11:64794735-64795043	NM_023479	+	Elac2
3	chr11:77993198-77993277	NM_080849	-	Nek8
4	chr11:83288585-83288722	NM_027427	+	Taf15
5	chr12:103105414-103105516	NM_172584	-	Itpk1
6	chr12:106085538-106085592	NM_029654	-	Atg2b
7	chr12:32240295-32240346	NM_028002	-	Dus4l
8	chr12:79146525-79146900	NM_172952	+	Gphn
9	chr14:53217284-53217366	NM_134076	+	Abhd4
10	chr15:42506135-42506307	NM_009640	-	Angpt1
11	chr19:5894405-5894532	NM_198634	-	Tigd3
12	chr1:194853747-194853802	NM_016851	+	Irf6
13	chr1:54971110-54971389	NM_031179	-	Sf3b1
14	chr3:31186236-31186297	NM_008857	+	Prkci
15	chr5:151918880-151919088	NM_027009	-	Rfc3
16	chr5:64247236-64247398	NM_145923	-	Rell1
17	chr6:113384903-113384994	NM_001033204	-	Rpusd3
18	chr6:113385048-113385098	NM_001033204	-	Rpusd3
19	chr6:50495518-50495648	NM_007808	-	Cycs
20	chr6:52644020-52644188	NM_025816	+	Tax1bp1
21	chr7:140733745-140733804	NM_022433	-	Sirt3
22	chr7:49113604-49113702	NM_175272	+	Nav2
23	chr8:114224600-114224650	NM_029005	-	Mlkl
Hypomethylated Genes				
1	Chromosomal Location	NCBI Gene ID	Strand	Gene Name
2	chr11:69582755-69583933	NM_029348	+	Zbtb4
3	chr11:74983924-74984203	NM_001098203	-	Hic1
4	chr11:97265254-97265841	NM_021493	+	4933428G20Rik
5	chr12:100367180-100367991	NM_146037	+	Kcnk13
6	chr12:32645084-32645694	NM_011158	-	Prkar2b
7	chr14:97052128-97052272	NM_007826	-	Dach1
8	chr15:57815009-57815757	NM_173862	+	Fam83a
9	chr16:17038159-17038410	NM_183287	-	2610318N02Rik
10	chr19:45071590-45072230	NM_001130526	+	Lzts2
11	chr19:9055606-9056056	NM_009643	+	Ahnak
12	chr1:59425522-59425959	NM_008057	+	Fzd7
13	chr2:33709866-33710173	NM_175184	-	Fam125b
14	chr3:95326210-95326329	NM_001024841	-	Gm128
15	chr5:124792476-124793230	NM_021430	-	Rilpl1
16	chr6:31494606-31495459	NM_013723	-	Podxl
17	chr6:54494795-54495286	NM_027268	-	Scrn1
18	chr6:72829966-72830792	NM_019715	-	Kcmf1
19	chr6:72885926-72886925	NM_001039392	-	Tmsb10
20	chr6:93878058-93878670	NM_001083321	-	Magi1
21	chr8:42539770-42539888	NM_001005865	-	Mtus1
22	chr8:42540093-42540333	NM_001005865	-	Mtus1
23	chr8:47708198-47709000	NM_007450	-	Slc25a4

* promoter regions includes 2000bp upstream and downstream of the transcriptional start site

Figure 6. *Dnmt* mRNA expression and global DNA methylation in the prostate of Dnmt1 hypomorphic mice.

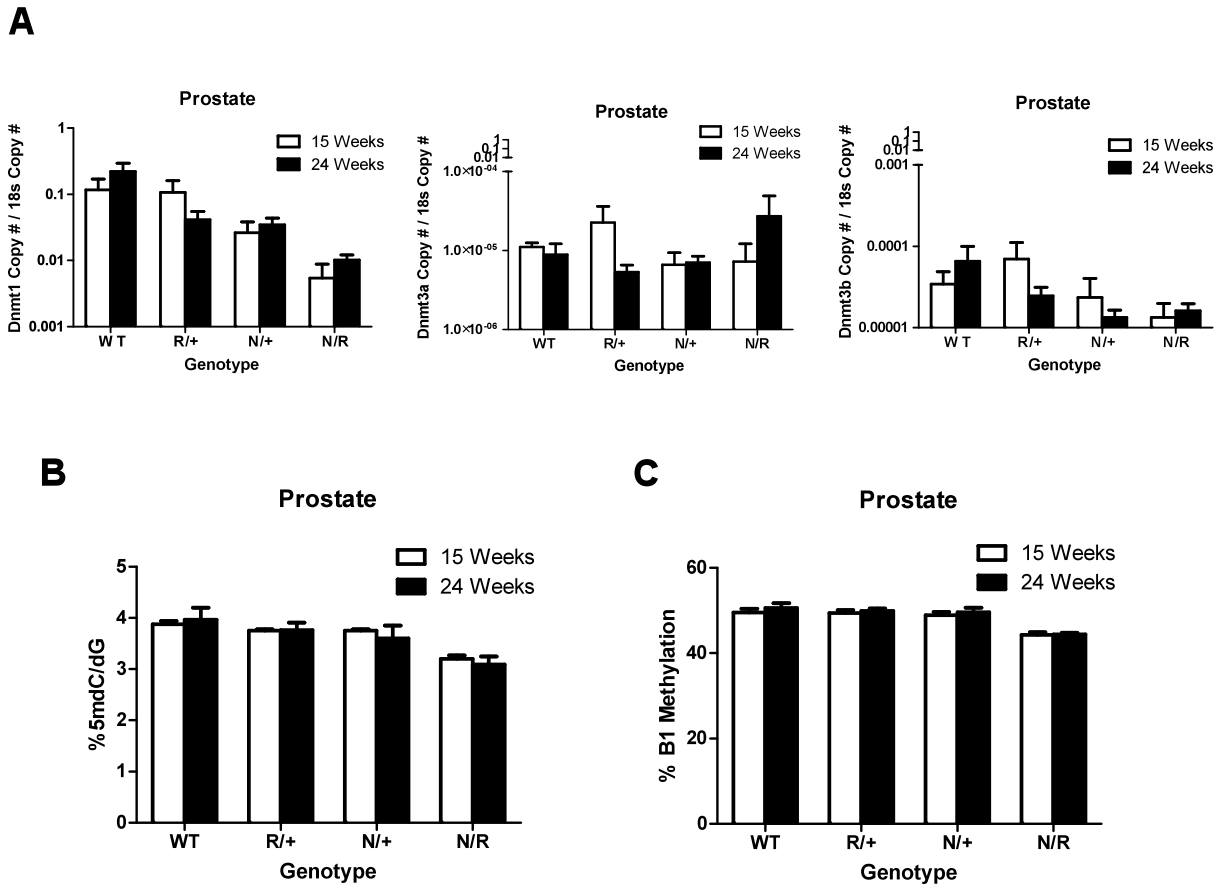

(*A*) *Dnmt1* (left), *Dnmt3a* (center), and *Dnmt3b* (right) mRNA expression in prostate tissues from mice of the indicated genotypes, at 15 and 24 weeks of age, were measured by qRT-PCR. Three to six mice were analyzed per group, and means and standard errors are plotted. (*B*) 5-methyl-deoxycytidine (5mdC) levels in prostate tissues from mice of the indicated genotypes, at 15 and 24 weeks of age, were measured by liquid chromatography-mass spectrometry (LC-MS). Three to four mice were analyzed per group, and means and standard errors are plotted. (*C*) B1 repetitive element methylation levels in prostate tissues from mice of the indicated genotypes, at 15 and 24 weeks of age, were measured by sodium bisulfite pyrosequencing. Three to four mice were analyzed per group, and means and standard errors are plotted.

Table 3. Inheritance of Dnmt1 hypomorphic alleles.

Genotype	WT	N/+	R/+	N/R
# Mice analyzed	53	46	49	8
Expected Mendelian Ratio	1	1	1	1
Observed Mendelian Ratio	1.1	0.9	1.0	0.2

- F1 offspring from cross of R/+ and N/+ C57BL/6 mice

Figure 7. Body and prostate weights of Dnmt1 hypomorphic mice.

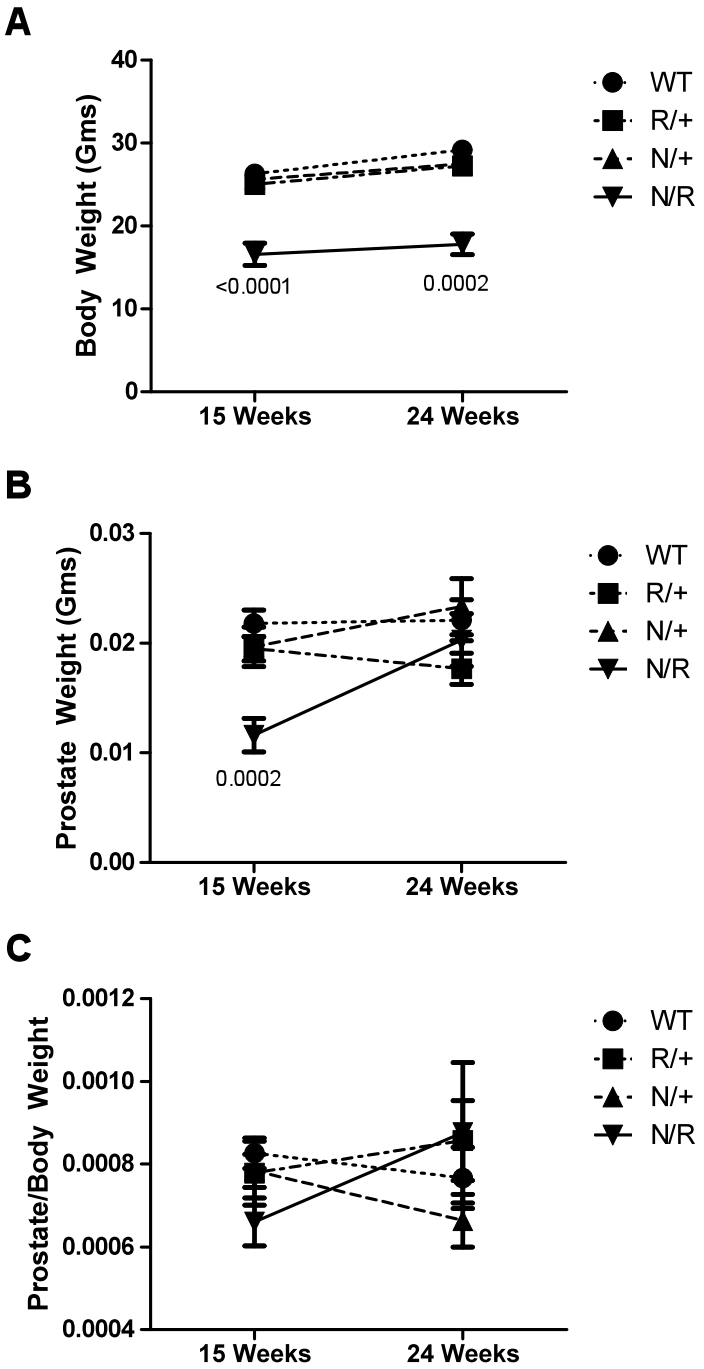

(*A*) Body weight of 15 and 24 week old mice of the indicated genotypes were determined at necropsy. (*B*) Prostate weight of 15 and 24 week old mice of the indicated genotypes were determined at necropsy. (*C*) Prostate weight normalized by body weight. Error Bars indicate standard error. Mann-Whitney test P values of significant differences, as compared to WT mice, are shown.

Figure 8. Prostate tissue architecture and differentiation marker expression in Dnmt1 hypomorphic mice.

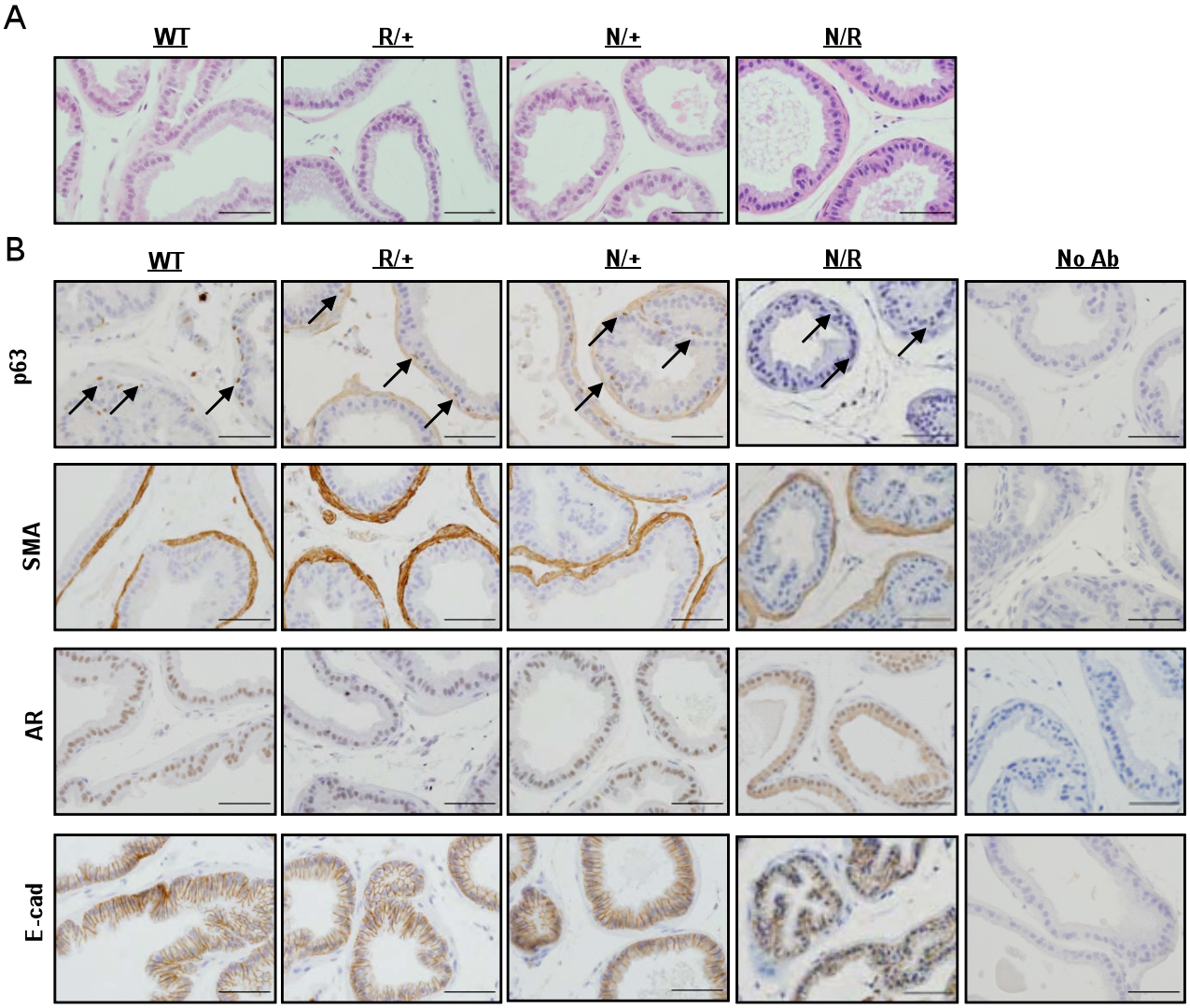

(*A*) H&E staining of lateral prostates from 15 week old mice of the indicated genotypes. (*B*) IHC staining of markers of prostate differentiation was performed on lateral prostates from 15 week old mice of the indicated genotypes. A no antibody control is shown at right. Staining is shown for p63 (basal cell marker), smooth muscle actin (SMA) (marker of the muscular layer surrounding glands), androgen receptor (AR) (marker for luminal epithelial cells, with predominantly nuclear staining), and E26 cadherin (marker for luminal epithelial cells, with predominantly plasma membrane staining). Magnification bar = 100 μM.

Figure 9. *Dnmt* mRNA expression in prostates of TRAMP Dnmt1 hypomorphic mice.

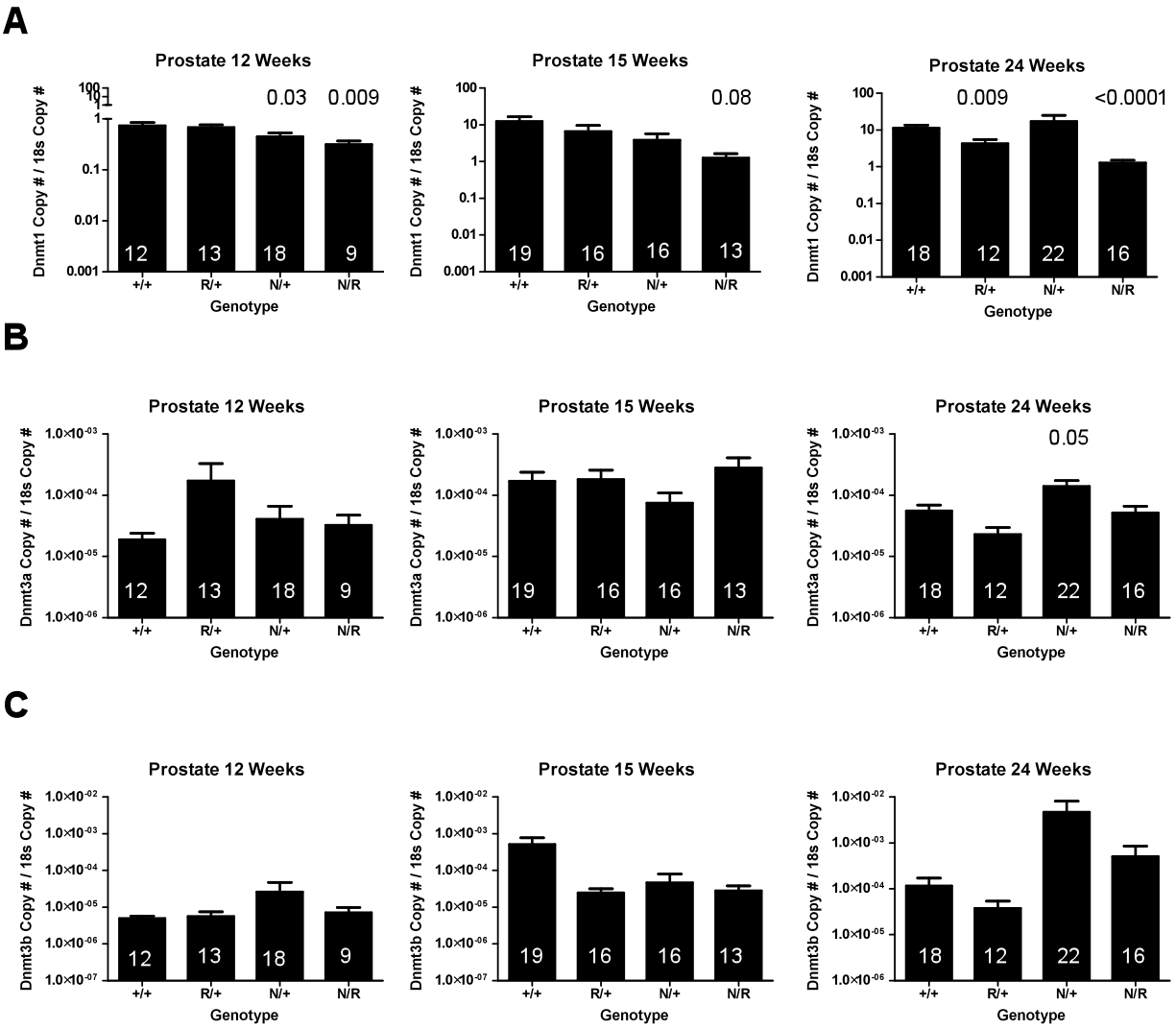

(*A*) *Dnmt1* mRNA expression in prostate tissues from mice of the indicated genotypes, at 12 (left), 15 (middle), and 24 (right) weeks of age, were measured by qRT-PCR. The number of samples analyzed per group is indicated in the columns, and means and standard errors are plotted. (*B*) *Dnmt3a* mRNA expression. (*C*) *Dnmt3b* mRNA expression. Mann-Whitney test P values of significant differences, as compared to TRAMP; +/+ mice, are shown.

Figure 10. Dnmt protein expression in prostates from TRAMP; Dnmt1 hypomorphic mice.

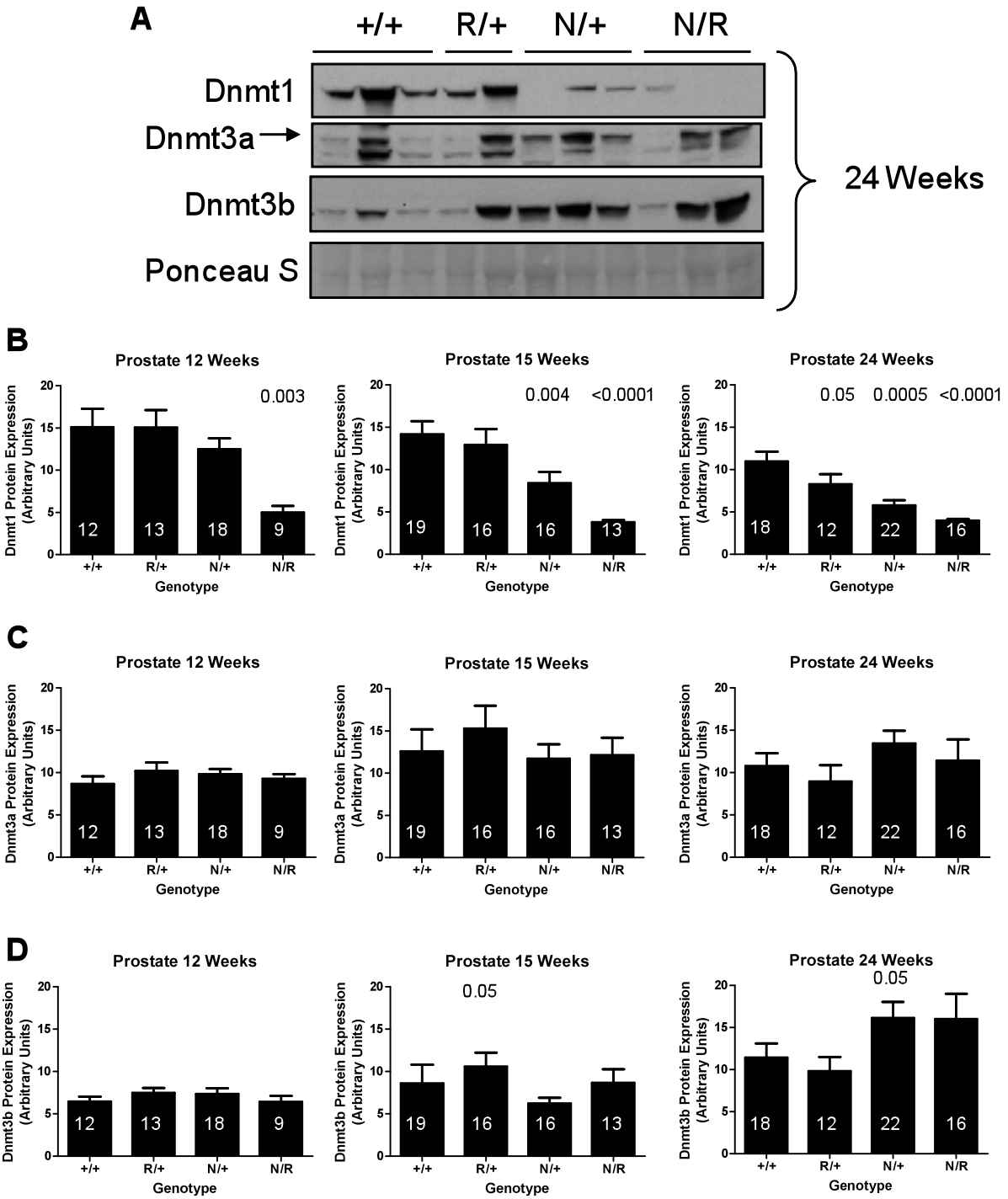

(*A*)Representative western blots of Dnmt1, Dnmt3a, and Dnmt3b in prostate tissues from 24 week old TRAMP mice of the indicated genotypes. The arrow indicates the position of Dnmt3a. Ponceau S staining was used to confirm equivalent protein loading. (*B*) Dnmt1 protein expression in prostate tissues from TRAMP mice of the indicated genotypes was determined by quantification of compiled western blot data. The left, middle, and right panels indicate expression data from 12, 15, and 24 week old mice, respectively. The number of samples analyzed per group is indicated in the columns, and means and standard errors are plotted. (*C*) Dnmt3a protein expression. (*D*) Dnmt3b protein expression. Mann-Whitney test P values of significant differences, as compared to TRAMP; +/+ mice, are shown.

Figure 11. IHC staining of Dnmt1 in the prostate of TRAMP Dnmt1 hypomorphic mice.

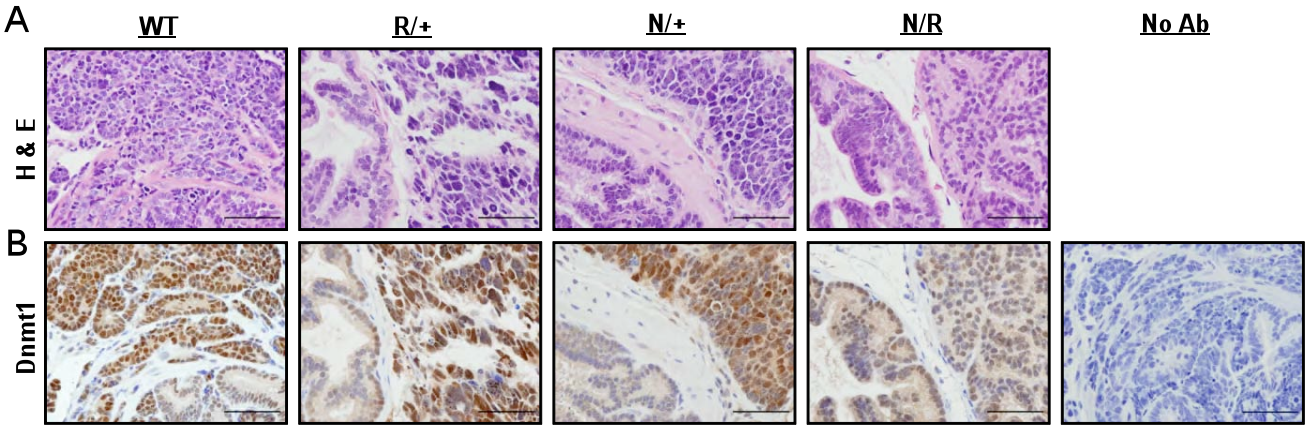

(*A*) H&E staining of lateral prostates from 24 week old TRAMP mice of the indicated genotypes was performed as described in the *Materials and methods*. (*B*) IHC staining of Dnmt1 performed on lateral prostates from 24 week old TRAMP mice of the indicated genotypes. Staining conditions are described in the *Materials and methods*, and a no antibody control is shown at right. Magnification bar = 100 µM.

Figure 12. Global DNA methylation in prostates of TRAMP Dnmt1 hypomorphic mice.

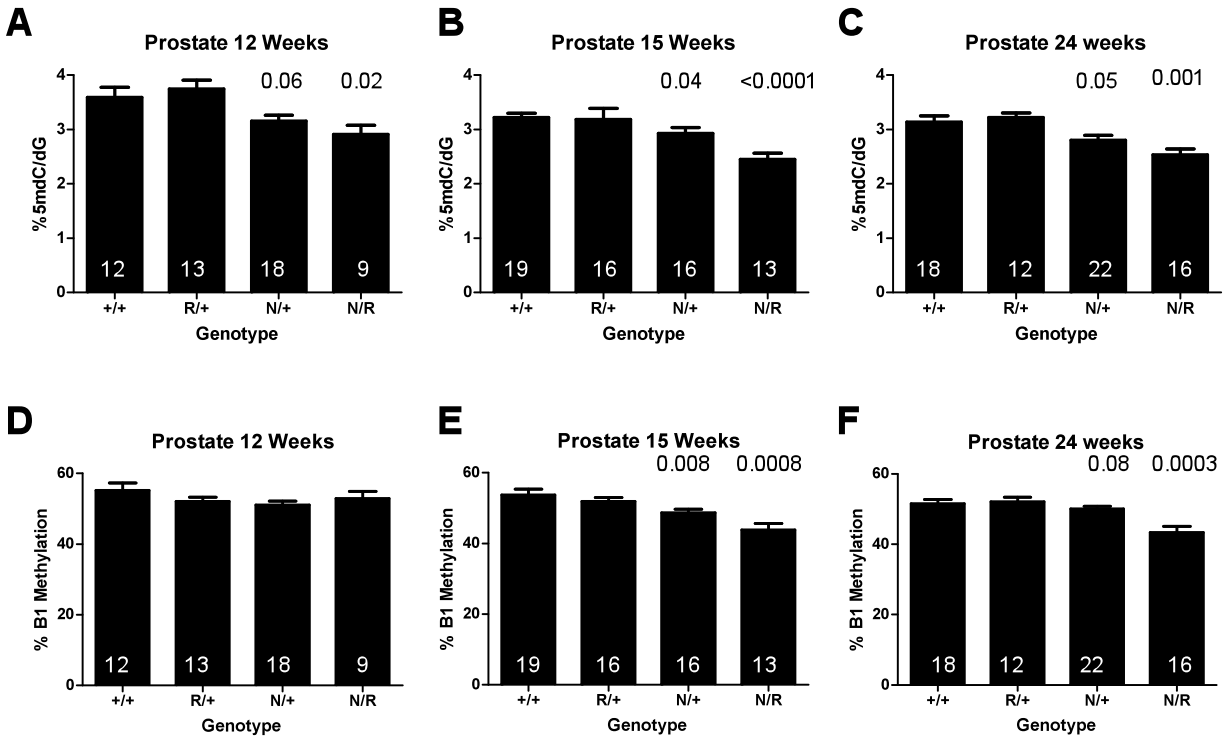

(*A*-*C*) 5-methyl-deoxycytidine (5mdC) levels in prostate tissues from TRAMP mice of the indicated genotypes, at 12 (*A*), 15 (*B*), and 24 (*C*) weeks of age, were measured by liquid chromatography-mass spectrometry (LC-MS). The number of samples analyzed per group is indicated in the columns, and the mean and standard errors are plotted. (*D*-*F*) B1 repetitive element methylation levels in prostate tissues from mice of the indicated genotypes, at 12 (*D*), 15 (*E*), and 24 (*F*) weeks of age, were measured by sodium bisulfite pyrosequencing. The number of samples analyzed per group is indicated in the columns, and the mean and standard errors are plotted. Mann-Whitney test P values of significant differences, as compared to TRAMP; +/+ mice, are shown.

Figure 13. Locus-specific DNA methylation in prostates from TRAMP Dnmt1 hypomorphic mice.

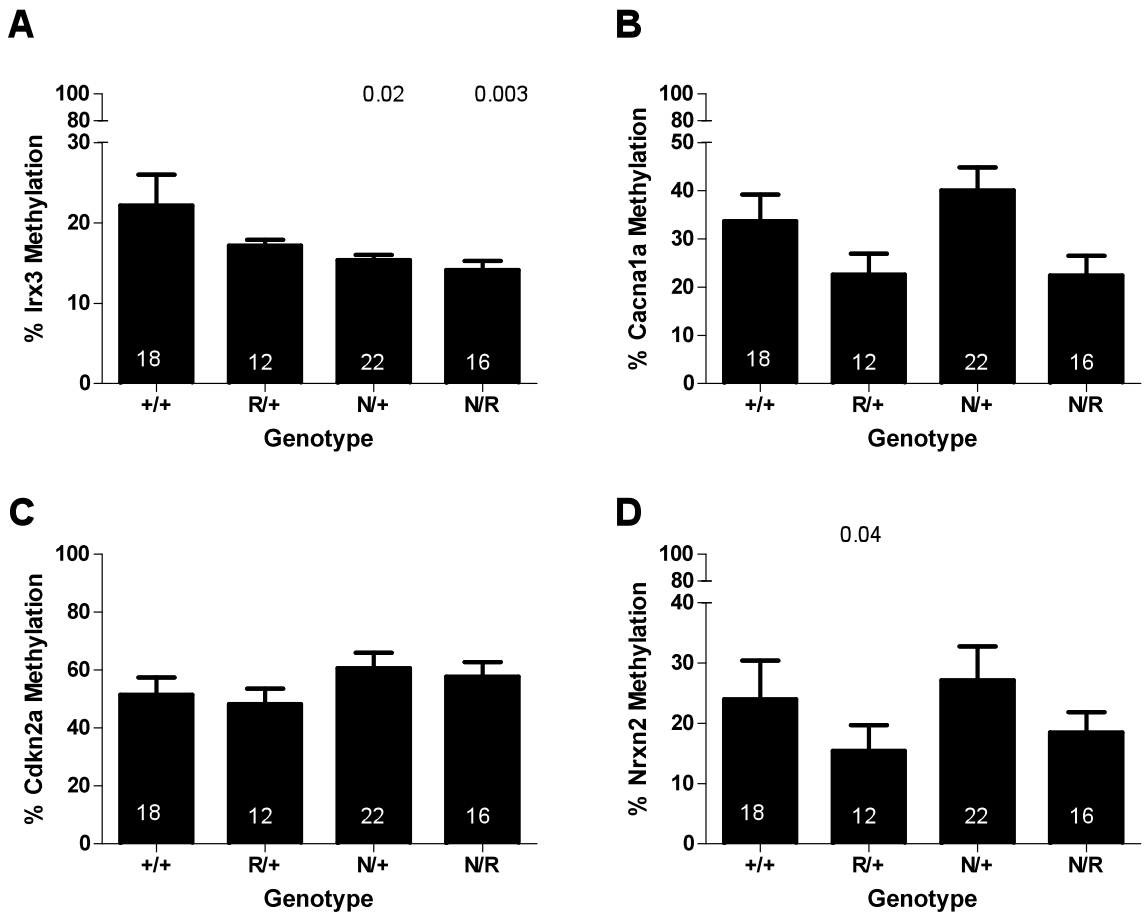

MAQMA was used to determine locus-specific DNA methylation in prostate tissues, from 24 week old TRAMP mice of the indicated genotypes. (*A*) *Irx3* 5' region methylation. (*B*) *Cacna1a* gene body methylation. (*C*) *Cdkn2a* gene body methylation. (*D*) *Nrxn2* gene body methylation. In each panel, the number of samples analyzed per group is indicated in the columns, and means and standard errors are plotted. Mann-Whitney test P values of significant differences, as compared to TRAMP; +/+ mice, are shown.

Table 4. Genes displaying significant promoter hypomethylation in TRAMP N/R prostate versus TRAMP +/+ prostate

#	Chromosomal location	NCBI gene ID	Strand	Gene
1	chr1:122430718-122430988*	NM_010133	+	En1
2	chr1:93229088-93229328	NM_023343	-	Ilkap
3	chr10:77755515-77755732	NM_053014	-	Agpat3
4	chr10:80025217-80025922	NM_134002	+	Csnk1g2
5	chr10:80672284-80672468	NM_018758	+	Apba3
6	chr10:82296563-82296766	NM_025499	+	Eid3
7	chr11:114490519-114490859	NM_053273	+	Ttyh2
8	chr11:45894537-45895757	NR_015372	-	Gm12166
9	chr12:87877254-87877436	NM_001080943	-	Zdhhc22
10	chr13:74070129-74070410	NM_146047	+	Clptm1l
11	chr13:74829399-74829633	NM_001033042	-	AI595366
12	chr14:102232151-102232473	NM_207215	-	Mycbp2
13	chr14:53570992-53571320	NM_011186	-	Psmb5
14	chr14:61714343-61714619	NM_008715	-	Ints6
15	chr15:39773624-39773901	NM_172814	-	Lrp12
16	chr15:98084696-98084941	NM_027304	-	H1fnt
17	chr16:21924600-21924858	NM_029457	+	Senp2
18	chr16:98116336-98116675	NM_001081684	-	Zfp295
19	chr17:24461083-24461296	NM_025425	+	Rpl3l
20	chr17:49655950-49656228	NM_181397	-	Rftn1
21	chr18:35752286-35752426	NM_011397	-	Slc23a1
22	chr19:56775604-56776431	NM_007419	+	Adrb1
23	chr19:61283175-61283297	NM_009970	-	Csf2ra
24	chr2:119366454-119366619	NM_030112	+	Rtf1
25	chr2:163610000-163610233	NM_183023	-	Rims4
26	chr2:163881277-163881596	NM_138684	-	Wfdc12
27	chr2:178336884-178337056	NM_177191	-	Sycp2
28	chr2:181423055-181423207	NM_183181	+	BC050777
29	chr3:124313792-124313987	NM_146140	+	Tram1l1
30	chr3:129190916-129191368	NM_011098	+	Pitx2
31	chr3:31285049-31285225	NM_001039090	+	Skil
32	chr4:125826514-125826653	NM_011902	-	Tekt2
33	chr4:126237642-126238056	NM_198960	-	Tcfap2e
34	chr5:147632069-147632410	NM_001039678	-	Prhoxnb
35	chr6:114096847-114097302	NM_172890	+	Slc6a11
36	chr6:149058727-149059188	NM_177192	-	Dennd5b
37	chr7:100536015-100536192	NM_013746	-	Plekhb1
38	chr7:102514864-102514974	NM_146325	+	Olfr554
39	chr7:143285311-143285490	NM_001042760	+	Slc22a18
40	chr7:18146202-18146431	NM_194064	+	Nanos2
41	chr7:28249740-28249950	NM_026716	+	Sycn
42	chr7:44336879-44337309	NM_025368	+	Josd2
43	chr7:45150175-45150462	NM_001033176	+	1700039E15Rik
44	chr7:45274741-45275022	NM_010596	+	Kcna7
45	chr7:75329248-75329459	NM_029332	+	Akap13
46	chr8:109985289-109985596	NM_001083118	-	Terf2
47	chr8:124464733-124465157	NM_133765	-	Fbxo31
48	chr8:28442989-28443225	NM_001101502	+	Zfp703
49	chr8:97218598-97218829	NM_019415	+	Slc12a3
50	chr9:14026649-14026935	NM_030261	+	Sesn3
51	chr9:14501507-14501718	NM_010242	-	Fut4
52	chrX:129821859-129822091	NM_028958	-	Taf7l
53	chrX:89927738-89928361	NM_211138	+	Pcyt1b

* Genes in bold were identified from 24 week old mice, the rest were from 15 week old mice

Table 5. Hypomethylation of Promoters versus Gene bodies in Dnmt1 hypomorphic mice

Region of Gene			% Decrease in N/R	
	WT-24	N/R-24		
Number of Fragments/Gene Body	278830	270651	0.03	2.93
Number of Fragments/Promoter	24377	26028	-0.07	-6.77
	TRAMP +/+-15	TRAMP N/R-15		
Number of Fragments/Gene Body	287237	273732	0.05	4.70
Number of Fragments/Promoter	26407	26296	0.00	0.42
	TRAMP +/+ -24	TRAMP N/R-24		
Number of Fragments/Gene Body	296091	277835	0.06	6.17
Number of Fragments/Promoter	39737	25325	0.36	36.27

Figure 14. Prostate weight and tumor incidence in TRAMP Dnmt1 hypomorphic mice.

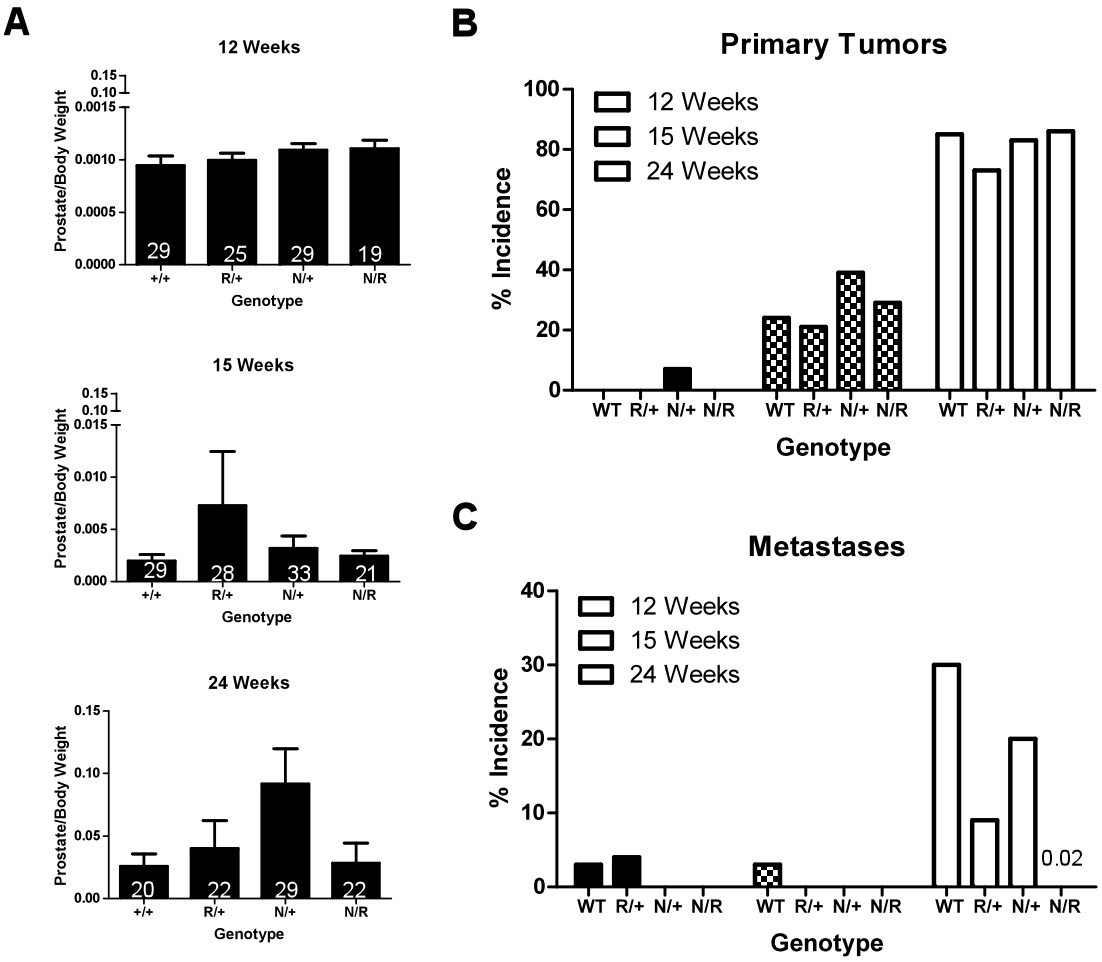

(*A*) Prostate weights (normalized to body weight) of TRAMP mice of the indicated genotypes were determined at necropsy at 12, 15, and 24 weeks of age (upper, middle, and lower graphs, respectively). The number of samples analyzed per group is indicated in the columns, and means and standard errors are plotted. (*B*) Primary tumor incidence of TRAMP mice of the indicated genotypes was determined at necropsy at 12, 15, and 24 weeks of age. Bars indicate the means of each sample group and the number of samples analyzed per group is the same as in (*A*). (*C*) Macro-metastatic tumor incidence of TRAMP mice of the indicated genotypes was determined at necropsy at 12, 15, and 24 weeks of age. Bars indicate the means of each sample group and the number of samples analyzed per group is the same as in (*A*). Fisher's exact test P values of significant differences, as compared to TRAMP; +/+ mice, are shown.

Figure 15. Prostate pathological stage and disease index in TRAMP Dnmt1 hypomorphic mice.

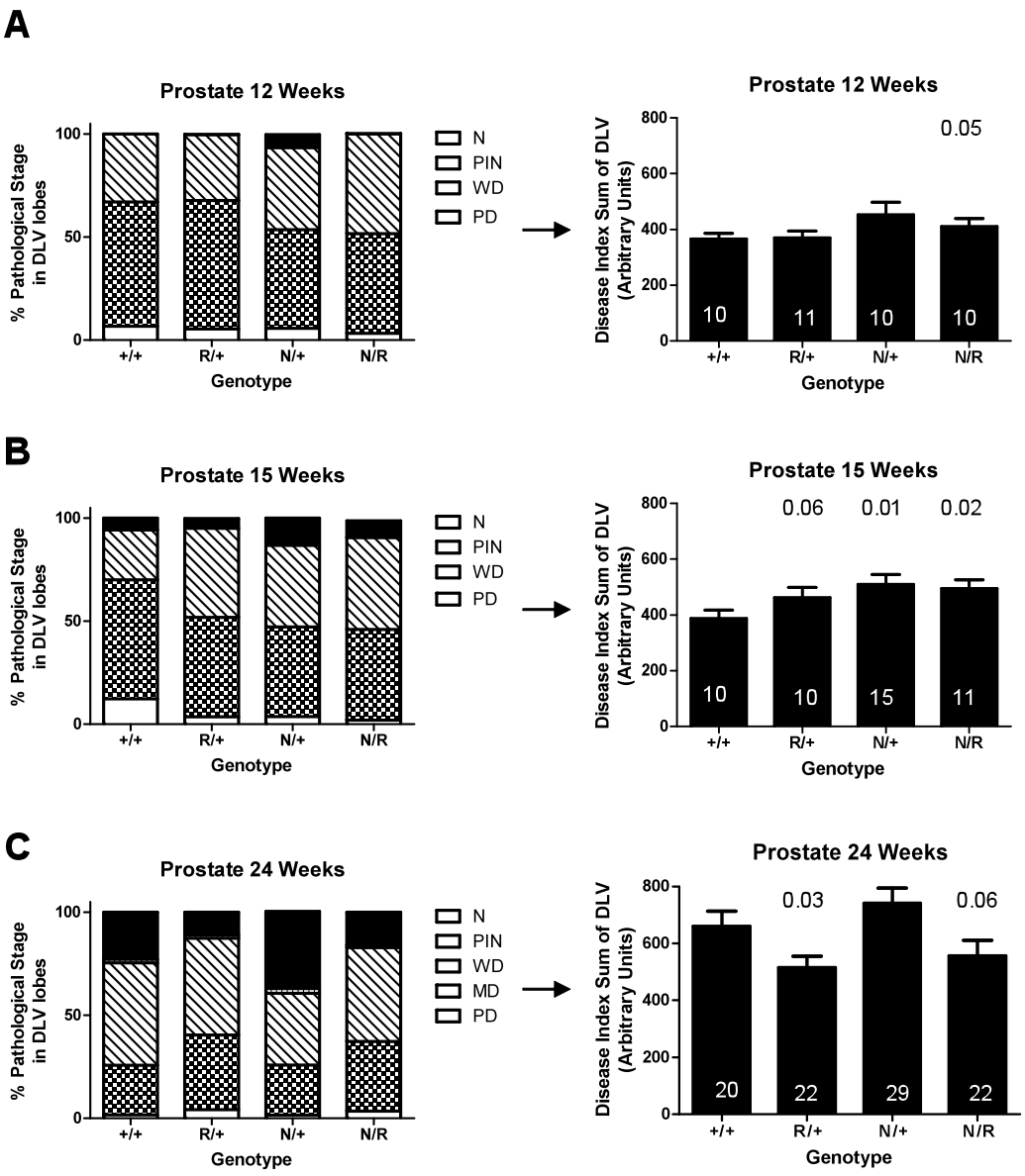

Pathological stage was determined for the dorsal, lateral, and ventral prostate lobes (DLV) and averaged. (*A*) The proportion of the prostate classified as normal (N), PIN, well-differentiated tumor (WD), and poorly differentiated tumor (PD) for mice of each TRAMP genotype, at 12 weeks of age, is plotted at left. The calculated disease index for the data set is shown at right. The number of samples analyzed per group is indicated in the columns, and means and standard errors are plotted. (*B*) Pathological staging and disease index calculation as described in (*A*), for 15 week old mice. (*C*) Pathological staging and disease index calculation as described in (*A*), for 24 week old mice. Mann-Whitney test P values of significant differences, as compared to TRAMP; +/+ mice, are shown.

Table 6. Tumor incidence in TRAMP; Dnmt1 hypomorphic mice

Genotype / Age at sac	N	Primary Tumor Incidence	Fisher's Exact p-value (vs. WT)	Total Metastatic Incidence	Fisher's Exact p-value (vs. WT)	Local or Distant Metastatic Incidence
+/+ / 12 weeks	N = 29	**0%**		**3%**		Local **0%** Distant **3%**
R/+ / 12 weeks	N = 25	**0%**	1.00	**4%**	1.0	Local **0%** Distant **4%**
N/+ / 12 weeks	N = 29	**7%**	1.00	**0%**	1.0	Local **0%** Distant **0%**
N/R / 12 weeks	N = 19	**0%**	1.00	**0%**	1.0	Local **0%** Distant **0%**
+/+ / 15 weeks	N = 29	**24%**		**3%**		Local **0%** Distant **3%**
R/+ / 15 weeks	N = 28	**21%**	0.74	**0%**	1.0	Local **0%** Distant **0%**
N/+ / 15 weeks	N = 33	**39%**	0.39	**0%**	1.0	Local **0%** Distant **0%**
N/R / 15 weeks	N = 21	**29%**	0.73	**0%**	1.0	Local **0%** Distant **0%**
+/+ / 24 weeks	N = 20	**85%**		**30%**		Local **15%** Distant **15%**
R/+ / 24 weeks	N = 22	**73%**	1.0	**9%**	0.11	Local **4.5%** Distant **4.5%**
N/+ / 24 weeks	N = 29	**83%**	1.0	**20%**	0.52	Local **17%** Distant **3%**
N/R / 24 weeks	N = 22	**86%**	1.0	**0%**	0.02	Local **0%** Distant **0%**

Table 7. Micrometastatic tumor incidence in TRAMP Dnmt1 hypomorphic mice[1]

Genotype / Age at Sac	Microscopic Metastatic Incidence		
+/+ / 12 weeks	N = 9	Local **0%**	Distant **0%**
R/+ / 12 weeks	N = 9	Local **0%**	Distant **0%**
N/+ / 12 weeks	N = 10	Local **0%**	Distant **0%**
N/R / 12 weeks	N = 10	Local **0%**	Distant **0%**
+/+ / 15 weeks	N = 10	Local **0%**	Distant **0%**
R/+ / 15 weeks	N = 9	Local **0%**	Distant **0%**
N/+ / 15 weeks	N = 15	Local **13%**	Distant **0%**
N/R / 15 weeks	N = 11	Local **9%**	Distant **0%**
+/+ / 24 weeks	N = 20	Local **40%**	Distant **15%**
R/+ / 24 weeks	N = 22	Local **23%**	Distant **9%**
N/+ / 24 weeks	N = 22	Local **50%**	Distant **5%**
N/R / 24 weeks	N = 22	Local **41%**	Distant **0%**